5-2012

Light detection and ranging (LiDAR) and multispectral studies of disturbed Lake Superior coastal environments

W. Charles Kerfoot
Michigan Technological University

Foad Yousef
Michigan Technological University

Sarah A. Green
Michigan Technological University

Robert Regis
Michigan Technological University

Robert Shuchman
Michigan Technological University

See next page for additional authors

Recommended Citation

Kerfoot, W. C., Yousef, F., Green, S. A., Regis, R., Shuchman, R., Brooks, C. N., Sayers, M., Sabol, B., & Graves, M. (2012). Light detection and ranging (LiDAR) and multispectral studies of disturbed Lake Superior coastal environments. *Limnology and Oceanography, 57*(3), 749-771. http://dx.doi.org/10.4319/lo.2012.57.3.0749

Retrieved from: https://digitalcommons.mtu.edu/mtri_p/11

Follow this and additional works at: https://digitalcommons.mtu.edu/mtri_p

 Part of the Oceanography Commons

Limnol. Oceanogr., 57(3), 2012, 749–771

doi:10.4319/lo.2012.57.3.0749

Light detection and ranging (LiDAR) and multispectral studies of disturbed Lake Superior coastal environments

W. Charles Kerfoot,[a,b,*] Foad Yousef,[a,b] Sarah A. Green,[c] Robert Regis,[d] Robert Shuchman,[d,e] Colin N. Brooks,[e] Mike Sayers,[e] Bruce Sabol,[f] and Mark Graves[f]

[a] Lake Superior Ecosystems Research Center, Michigan Technological University, Houghton, Michigan
[b] Department of Biological Sciences, Michigan Technological University, Houghton, Michigan
[c] Department of Chemistry, Michigan Technological University, Houghton, Michigan
[d] Department of Geological and Mining Engineering and Sciences, Michigan Technological University, Houghton, Michigan
[e] Michigan Tech Research Institute, Ann Arbor, Michigan
[f] U.S. Army Engineer Research and Development Center (ERDC-Environmental Laboratory), Vicksburg, Mississippi

Abstract

Due to its high spatial resolution and excellent water penetration, coastal light detection and ranging (LiDAR) coupled with multispectral imaging (MSS) has great promise for resolving shoreline features in the Great Lakes. Previous investigations in Lake Superior documented a metal-rich "halo" around the Keweenaw Peninsula, related to past copper mining practices. Grand Traverse Bay on the Keweenaw Peninsula provides an excellent Great Lakes example of global mine discharges into coastal environments. For more than a century, waste rock migrating from shoreline tailings piles has moved along extensive stretches of coast, damming stream outlets, intercepting wetlands and recreational beaches, suppressing benthic invertebrate communities, and threatening critical fish breeding grounds. In the bay, the magnitude of the discarded wastes literally "reset the shoreline" and provided an intriguing field experiment in coastal erosion and spreading environmental effects. Employing a combination of historic aerial photography and LiDAR, we estimate the time course and mass of tailings eroded into the bay and the amount of copper that contributed to the metal-rich halo. We also quantify underwater tailings spread across benthic substrates by using MSS imagery on spectral reflectance differences between tailings and natural sediment types, plus a depth-correction algorithm (Lyzenga Method). We show that the coastal detail from LiDAR and MSS opens up numerous applications for ecological, ecosystem, and geological investigations.

Light detection and ranging (LiDAR) is an airborne laser-ranging technique that acquires high-resolution elevation and bathymetric data (Ackermann 1999). The data are collected with aircraft-mounted lasers capable of recording elevation measurements at a rate of 10–200-kHz pulses s^{-1} for above-water topographic stretches and 1–10-kHz for coastal bathymetric surveys, with a maximum vertical precision of 15 cm (Crow et al. 2007). In coastal surveys, the aircraft travels over a water stretch at about 60 m s^{-1}, pulsing two varying laser beams toward earth through an opening in the plane's fuselage: a red wavelength (infrared) beam that is reflected by the water surface and a narrow, blue-green wavelength beam that penetrates the water surface and is reflected from the bottom surface. The LiDAR sensor records the time difference between the two signals to derive measurements of water depth.

An infrared version of LiDAR is used in forest applications, principally for biomass surveys and profiling of canopies (Lefsky et al. 1999). More recently, attention has expanded to underwater marine and freshwater applications. Under ideal conditions in coastal waters, blue-green laser penetration allows detection of structures down to depths approximately three times greater than passive light reflection. LiDAR has penetrated to a recorded maximum of 35 m in oceanic environments (Guenther 2007). Applications of blue-green laser techniques to mapping underwater structures have recently expanded. Marine studies include mapping of coral reefs (Brock et al. 2004), characterization of Atlantic barrier islands (Nayegandhi et al. 2005), and studies of Gulf of Mexico estuaries (Brock et al. 2002). In freshwater applications, recent river channel-bed characterizations include erosional surveys along braided streams (Bowen and Waltermire 2002). Here we emphasize potential applications in the Great Lakes and marine coastal environments, particularly under circumstances where past and present mine tailings discharges or tailings pond failures are of concern.

Multispectral sensors (MSS) are instruments that acquire passive reflectance images in many continuous spectral bands throughout the visible, near-infrared, mid-infrared, and thermal portion of the spectrum. These systems can discriminate above- and below-water surface features that have diagnostic absorption and reflectance characteristics. In our case, keying off albedo and spectral differences, they were used jointly with LiDAR to characterize stamp sand dispersal along the shoreline and under the water.

Studies were carried out along the southern shoreline of Lake Superior, on the Keweenaw Peninsula. Recent investigations in Lake Superior documented a metal-rich "halo" around the Keweenaw Peninsula associated with past copper mining practices (Fig. 1; Kerfoot et al. 2004, 2009; Gewurtz et al. 2008). In Grand Traverse Bay (Fig. 2),

* Corresponding author: wkerfoot@mtu.edu

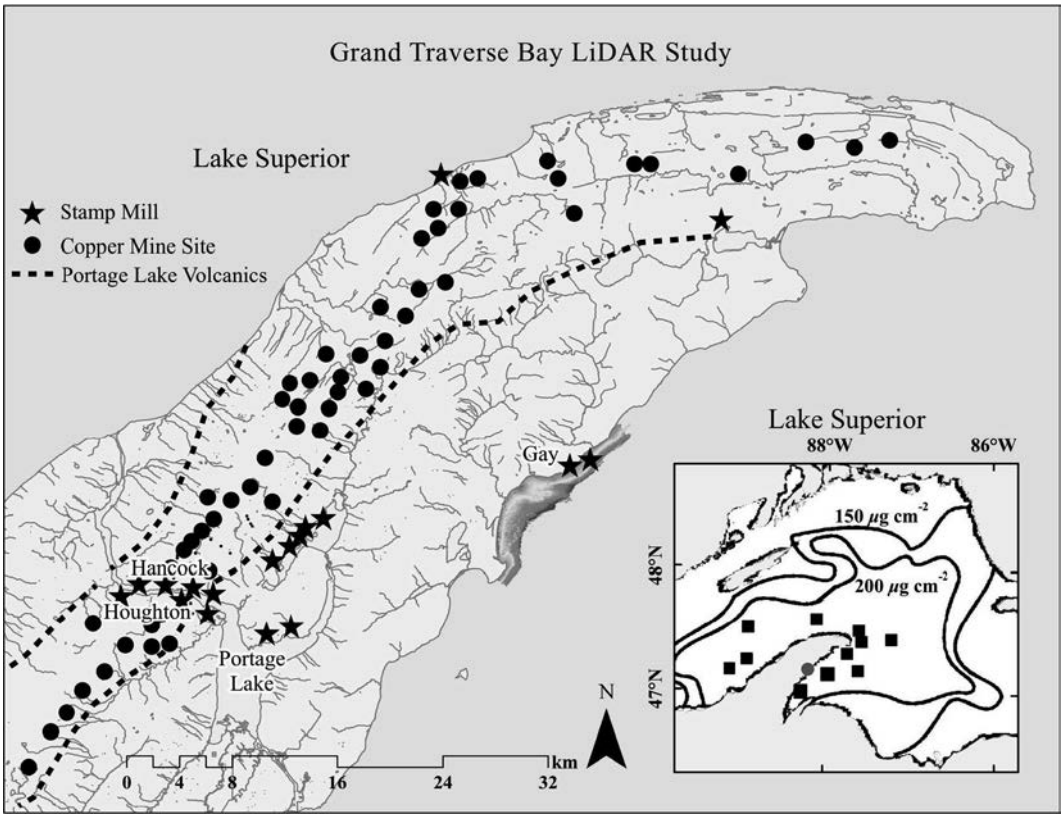

Fig. 1. Geographic location of Grand Traverse Bay (gray), on the Keweenaw Bay side of the Keweenaw Peninsula, along the southern shoreline of Lake Superior. The boundary of the Portage Lake Volcanics is indicated by dashed lines, copper mines by black dots, and shoreline stamp mills by black stars. Contours in Lake Superior represent copper inventory values (specific core sites from the NSF Keweenaw Interdisciplinary Transport Experiment in Superior KITES: solid black squares indicate 200–400 μg cm^{-2}; Kerfoot et al. 2004).

the magnitude of the discarded wastes literally "reset the shoreline" and provided an intriguing field experiment. We used the Compact Hydrographic Airborne Rapid Total Survey (CHARTS) system, one that collects LiDAR and multispectral scanner Compact Airborne Spectrographic Imagery (CASI), to construct detailed coastal maps. Using a combination of historic aerial photography and LiDAR, we estimated the time course and amount of tailings that eroded into Keweenaw Bay and the quantity of copper that contributed to the metal-rich halo.

The Keweenaw Peninsula was one of the first great metal mining regions in North America. Between 1850 and 1929, the district was the second largest producer of copper in the world (Murdoch 1943; Benedict 1952). Native copper in the Portage Lake Volcanic Series came from two principal kinds of ore: basalt lava flows (amygdule deposits) and inter-bedded sediments (conglomerates). Both were crushed with early gravity and later giant steam-driven stamps to release the native copper and silver (Butler and Burbank 1929; Benedict 1955). During that interval, mill sites and stamp sand piles dotted the regional landscape (Fig. 1). More than 140 mines worked the central deposits and > 40 mills processed stamp rock (Kerfoot et al. 1994). The unit used here to express mass is the teragram (Tg), equivalent to 10^{12} grams or 1 megatonne (Mt). Smelters produced 4.4 Tg of copper, while stamp mills sluiced around 360 Tg of copper-rich stamp tailings into rivers and waterways, including 64 Tg directly onto Lake Superior shorelines and 25 Tg into Keweenaw Bay (Kerfoot et al. 1994, 2009; Kolak et al. 1999).

In Grand Traverse Bay, the magnitude of the wastes initiated a perturbation that has played out for more than a century. The coastal stamp sands in the bay were promising for CHARTS studies because albedo and spectral reflectance contrasts between stamp sands and natural sediments afforded opportunities to locate drift of tailings over natural coastal sediments (Fig. 3a,b). Here we emphasize that LiDAR and MSS applications have a wide range of uses. These include: (1) identifying drifting sediment inputs from multiple sources (e.g., tailings, shoreline dunes, gravel or cobble beds, river-mouth sediments); (2) characterizing post-Pleistocene features (e.g., Nipissing beach ridges, ancient riverbeds); and (3) quantifying substrate cover from seasonal biological variables (e.g., wetland vegetation, aquatic macrophytes, benthic cover). All these attributes are evident in the Grand Traverse Bay investigation. Yet we must also emphasize that coastal mine tailings, either from direct discharges or from failed tailings dams, are not just local curiosities, they present a genuine global problem (Martinez-Frias 1997; Macdonald et al. 2003).

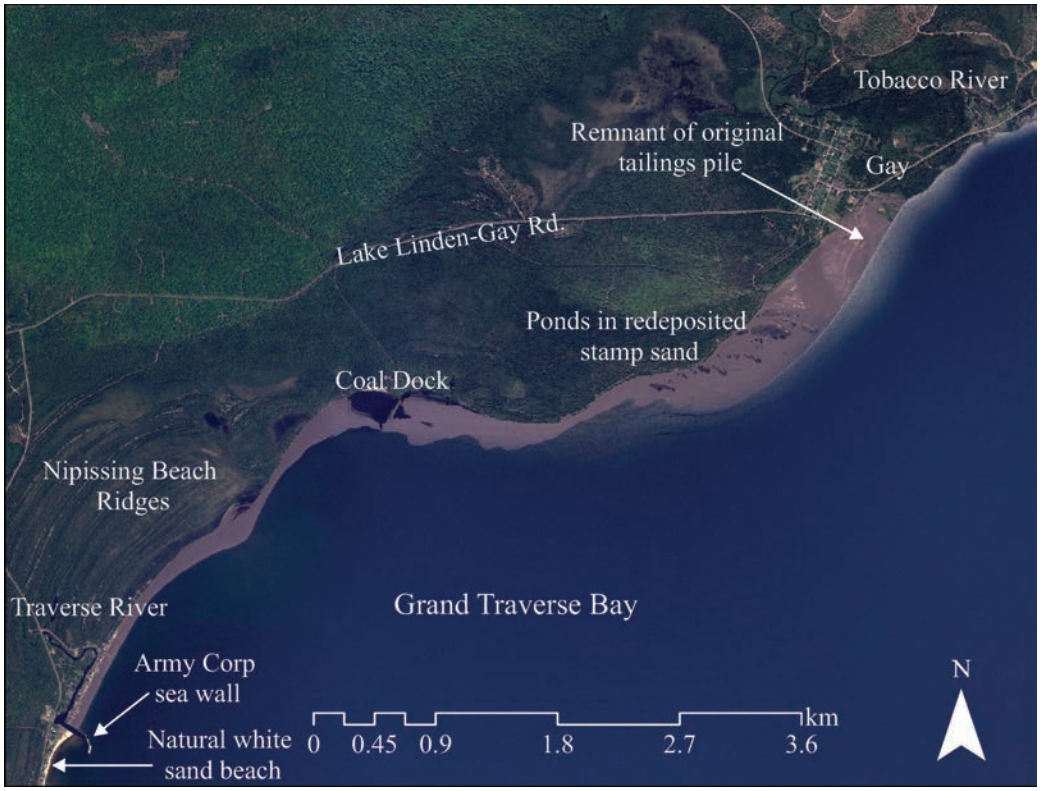

Fig. 2. Aerial image of Grand Traverse Bay (2005 National Photography Program, MrSID format). Labels indicate local features, including the original tailings pile remnant at Gay, the Coal Dock region, and redeposited stamp sand stretching southward to natural white sands at the Traverse River seawall. Note remnants of natural beach sands behind the Coal Dock and high on the beach north of the Traverse River seawall.

Methods

Determining discharges into Keweenaw Bay—The Copper Country Archives section of the J. R. Van Pelt Library, Michigan Technological University, retains copies of processing records from mining companies. The archived records include yearly reports of total copper produced, total amount of rock removed, total amount of stamp rock shipped to stamp mills, and operation details. The tallies allowed us to reconstruct accurate totals for yearly stamp stand discharges from mills into Keweenaw Bay (Table 1).

Estimating erosion of the Gay tailings pile after 1938—Material in the original stamp sand pile consisted of two fractions: a coarse fraction (sand) with a specific gravity around 2.9, and a fine silt-clay fraction (the so-called "slime clays"; Benedict 1955). Coarse grain sizes on tailings piles are angular, approximately log-normally distributed, with modal sizes ranging between 0.3 and 3.4 mm (Babcock and Spiroff unpubl.; Jeong et al. 1999). Prevailing coastal currents off Gay move strongly southward, with only occasional reversals (Chen et al. 2001; Zhu et al. 2001). Currents are maximum during late fall and early winter storms (60–80 cm s^{-1}; November to early December, National Oceanic and Atmospheric Administration [NOAA] Great Lakes Environmental Research Laboratory and Coastal Current Forecast Model, 2010). During wave erosion, the coarse fraction is redeposited as a beach sand to the south of the main pile (Fig. 2), whereas the fine silt-clay fraction (an estimated 7–14% of pile mass; Babcock and Spiroff unpubl.) is winnowed out and dispersed far out across the coastal shelf. The tailings are distinctively different in color, mineral content, and physical characteristics from the natural beach and lake sediments, derived from the local Jacobsville Sandstone formation.

LiDAR was used in this project principally for producing digital elevation models (DEMs). During the week of 23 June 2008, CHARTS aerial overflights of the Grand Traverse Bay area were performed by the Joint Airborne LiDAR Bathymetry Technical Center of Expertise. The pulse rates were 1 kHz at 532 nm and 9 kHz at 1064 nm with a scan width of -40° side to side from an altitude of 400 m. The flight speed was 125 knots (64 m s^{-1}), slower than normal for improved image collection. The preprocessed CHARTS LiDAR and 8-band multispectral data were forwarded to Michigan Technological University, Houghton, Michigan, and to Michigan Tech Research Institute, Ann Arbor, Michigan. Using the Geographic Information System (GIS)-referenced high-resolution LiDAR DEM portion of the data set, we constructed 2-m^2-resolution LiDAR bathymetry maps. The CHARTS LiDAR had a vertical resolution of 30 cm. At the same time, locations and orientation of the laser source were determined by the Geographic Positioning System and by the Internal Measurement Units, respectively.

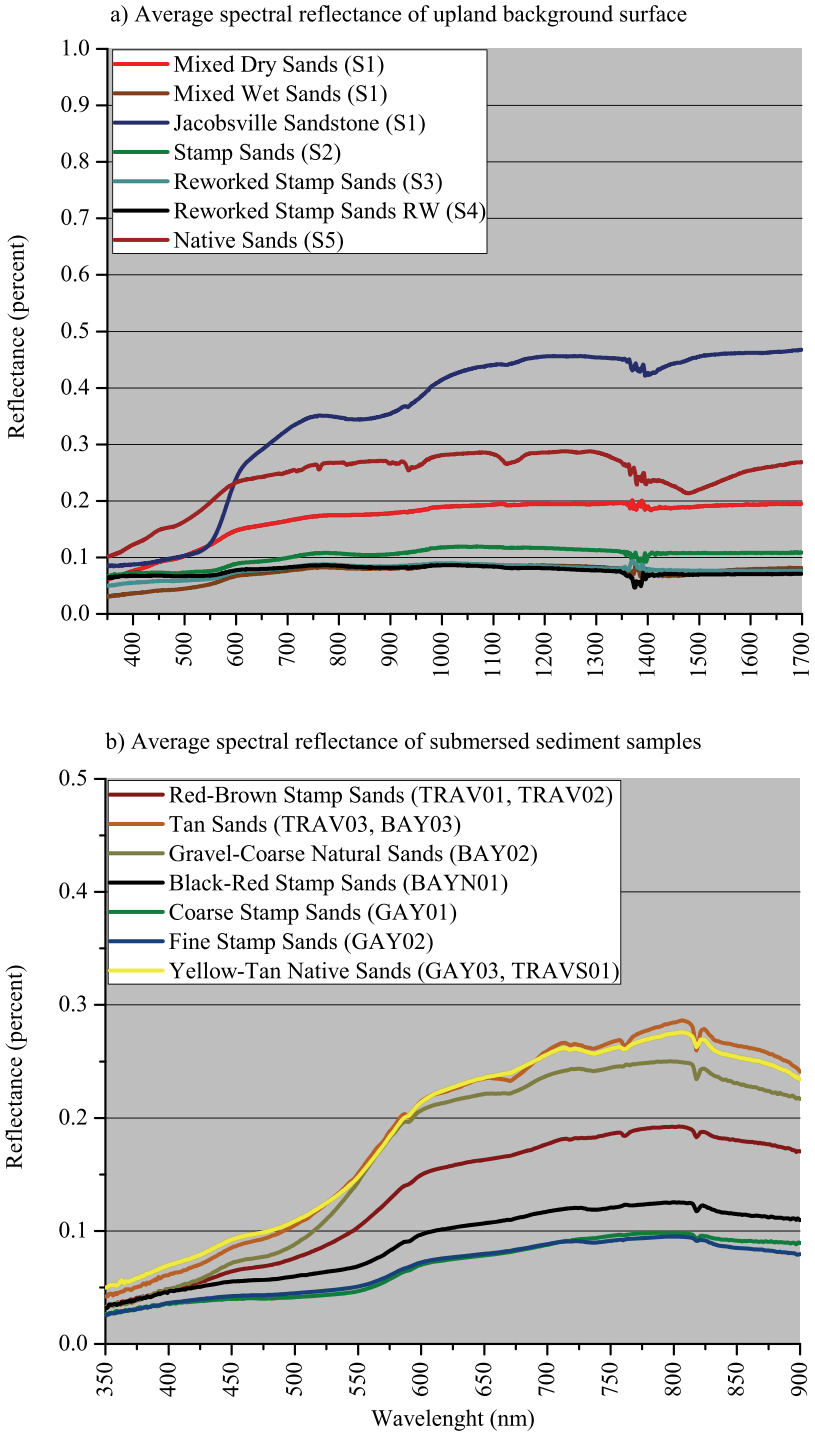

Fig. 3. (a) Spectral reflectance of shoreline above-water surfaces near Gay. Jacobsville Sandstone has the highest reflectance, whereas native beach sands have intermediate reflectance and stamp sands have the lowest reflectance. Native and stamp sand mixtures have intermediate reflectance values. (b) Spectral reflectance of submersed (1–2-cm) sediment samples collected from the Gay site. Yellow, tan, and gray natural sands show the highest spectral reflectance values, whereas coarse and fine stamp sands from Gay show the lowest. Note that the wavelength scale is shortened.

Table 1. Copper mill yearly discharges of stamp sands into Keweenaw Bay. Totals compiled from company records (Copper Country Archives, J. R. Van Pelt Library, Michigan Technological University, Houghton, Michigan).

Date	Mass Mill (Tg)	Mohawk Mill (Tg)	Wolverine Mill (Tg)
1898	0	0	0
1899	0	0	0
1900	0	0	0
1901	0	0	0
1902	152,562	7813	253,091
1903	122,611	261,645	284,912
1904	105,614	416,506	291,917
1905	143,430	531,837	310,065
1906	185,789	561,080	312,099
1907	204,599	581,249	316,451
1908	171,268	622,110	338,978
1909	139,404	742,932	354,528
1910	90,747	727,981	352,387
1911	73,475	727,991	364,026
1912	132,891	714,741	352,410
1913	78,250	332,414	165,207
1914	209,354	589,297	360,676
1915	323,335	752,702	352,769
1916	287,900	602,811	320,066
1917	244,671	548,979	275,303
1918	196,456	412,089	270,397
1919	123,780	508,642	233,391
1920	0	394,578	238,615
1921	0	624,332	263,439
1922	0	464,792	221,614
1923	0	367,749	86,545
1924	0	637,269	186,344
1925	0	580,607	39,607
1926	0	654,079	0
1927	0	689,285	0
1928	0	595,728	0
1929	0	562,026	0
1930	0	428,716	0
1931	0	402,698	0
1932	0	196,467	0
1933	0	0	0

For a check on the accuracy of bathymetric measurements, the LiDAR-derived depths were compared with georegistered National Water Resources Institute (NWRI) sonar-derived depths (Bieberhofer and Prokopec 2008). Statistical software packages (SYSTAT) were used for determining spatial cross-correlations. The resulting regression matches were very similar (Fig. 4b, $R^2 = 0.98$). Notice, however, that LiDAR in 2008 showed slightly less substrate depth in very shallow regions, compared to the 2004 sonar data set. The slight disparity may be real, as the NWRI depth data were collected 4 yr earlier. During the interval, migrating coastal stamp sands might have filled in more of the shallow depths.

Using CHARTS LiDAR data along with several aerial photos from 1938 to 2010, we attempted to reconstruct the 1938 Gay stamp sand pile volume and, with some reasonable assumptions, to calculate the shoreline erosion rate of the pile between 1938 and 2008, concluding with the year of the CHARTS overflight. To measure erosion of the tailings pile and the mass of sands washed into Lake Superior, three estimates were needed: (1) the area and volume of the pile above water level (available from the 2008 LiDAR); (2) the below-water volume, i.e., calculating the true depth of the stamp sand pile above lake bottom bedrock; and (3) the area of the pile lost through time (erosion at the shoreline face, estimated from aerial photos, essentially treated as vertical slices across the pile; Fig. 5).

Although discharges ended in 1932 (Fig. 6), the original boundaries of the Gay tailings pile were determined from a georegistered 1938 aerial photograph of the region. ArcMap9.3 was used to digitize this aerial photo (Jensen 2004). Wave action along the outer edge erodes the pile, yet the high specific gravity and angular nature of particles helps maintain a near-vertical face along the eroding cliff (Fig. 7a). Strong prevailing currents (Lam 1978; Chen et al. 2001; 2010 NOAA Great Lakes Environmental Research Laboratory Now-cast Wind Model) transported stamp sand particles southwestward, covering natural Jacobsville Sandstone outcrops and white beach sands. Seven other aerial photos, taken between 1944 and 2010, provided subsequent shoreline edge changes on the original tailings pile and estimates of redeposition along southern beaches, both quantified with ArcGIS and ENVI (Jensen 2004). The photos allowed mapping of the original pile's changing boundaries (Fig. 8), to which we fit pixel polygons.

To estimate below-water volume, the pile was separated into two regions. One region was the portion of the pile eroded to bedrock, which allowed LiDAR-derived estimates of past bottom contours under the original pile, whereas the second portion was the remaining part covered by stamp sand. In the first portion (eroded area), we assumed a fairly constant yearly water level (183.4 m; Detroit District Corps) to estimate the underwater volume of the pile. To estimate the depth of the stamp sand in the second region, currently covered by stamp sand, we used the slope change of bedrock from the LiDAR bathymetric map adjacent to the pile and extrapolated this slope under the pile. The result of the linear slope analysis produced an average depth below lake level of about 2 m for the currently covered portion.

To estimate volume lost above water (i.e., exposed shoreline component), we also needed to determine the elevation of the stamp sand pile removed by shoreline erosion. Again we considered the same two regions: current pile and the portion of the pile that was lost. The high-resolution 2008 LiDAR DEM provided the height measurement of the 2008 pile. Past pile elevations were reconstructed by extending the height of known existing landmarks (ends of preserved sluiceways) across the aerial photos to estimate depth. Photos and company discussions of the surface sluiceways suggested that most of the original Mohawk–Wolverine pile had been nearly flat, giving the tailings pile a flat-topped mesa, or table, appearance (Fig. 7b). The idea of a nearly flat slope (low grade) was compatible with conveyor belt operation. A very slight slope allowed extension as far as possible away from the mine and into Grand Traverse Bay. The average height of the above-water-level (8 m) portion and down-gradient

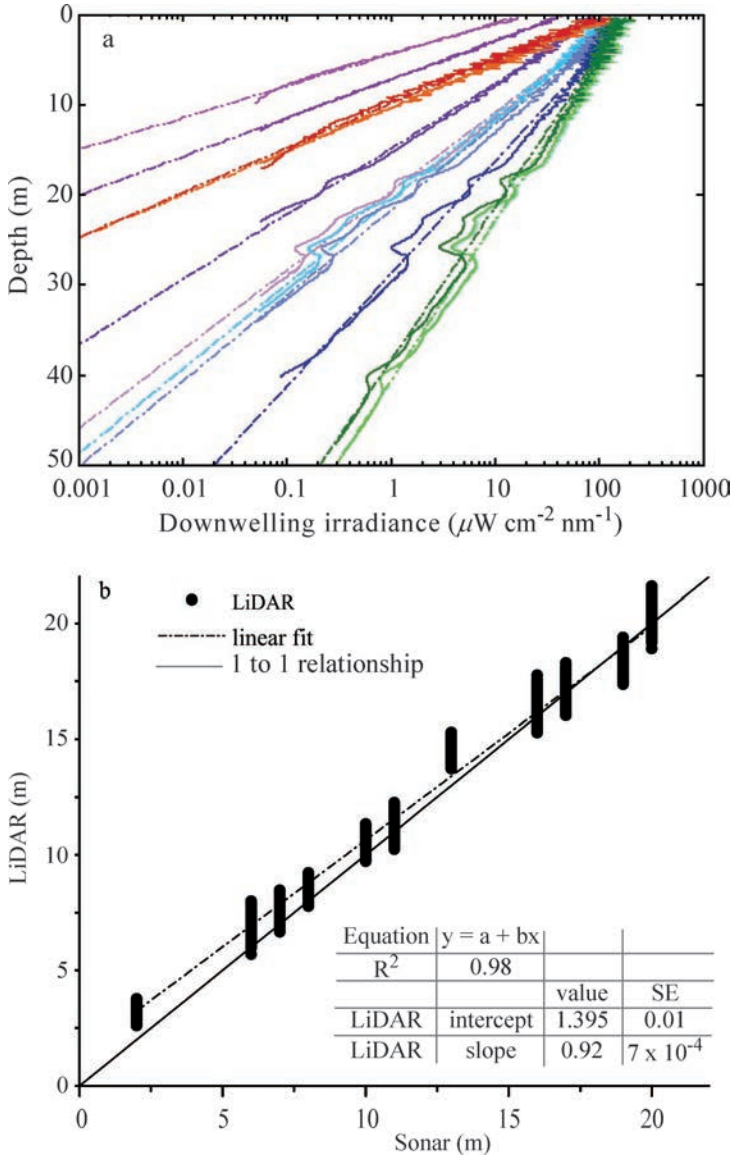

Fig. 4. (a) Sample data from Satlantic OC P1000 Optical Profiling Radiometer; each color represents a different spectral band. The dashed straight lines represent spectral regression lines using the Beer–Lambert's law equation. Notice how blues and greens (right lines) penetrate deeper than red wavelengths. (b) Regression of LiDAR-derived (2008 CHARTS) depths on sonar-derived (2004 NWRI) depths. Solid line represents a perfect match; dashed line is a linear data-fit line.

slope was determined from the 2008 LiDAR elevation values along the preserved sluiceway landmarks on the existing pile. Projected extension of the sluiceways was used to estimate the height of eroded portions, and past aerial photos to estimate area dimensions. The underwater volume was added based on estimated depth to bedrock.

The reconstructed pile was first used to calculate the volume and mass of stamp sand in 1938. Procedures employed a pixel spatial resolution of 3 m and an area of 9 m^2. Multiplying area by depth gave an estimate of volume of stamp sand for each pixel. Integration provided an estimate of total volume in cubic meters. An average of Colin's (internal report 2009; accessible from the U.S. Department of Agriculture's [USDA] Natural Resource Conservation Service) Web Soil Survey values (http://soildatamart.nrcs.usda.gov/Manuscripts/MI605/Keweenaw_MI.pdf) was used to assign mass. Moist bulk density of the Gay stamp sands soil was estimated as between 1.35–1.65 g cm^{-3} or 1350–6150 kg m^{-3}. We chose the mean bulk density value of 1.65 g cm^{-3} and calculated the mass for each eroded slice. An exponential decay equation was fit to the mean erosion curve, giving an intercept estimate of date when the pile was gone (i.e., zero mass). A separate independent estimate of zero mass intercept came from log-transformed values, after fitting a line to the linear points. However, because of log-transformation, that line estimated loss based

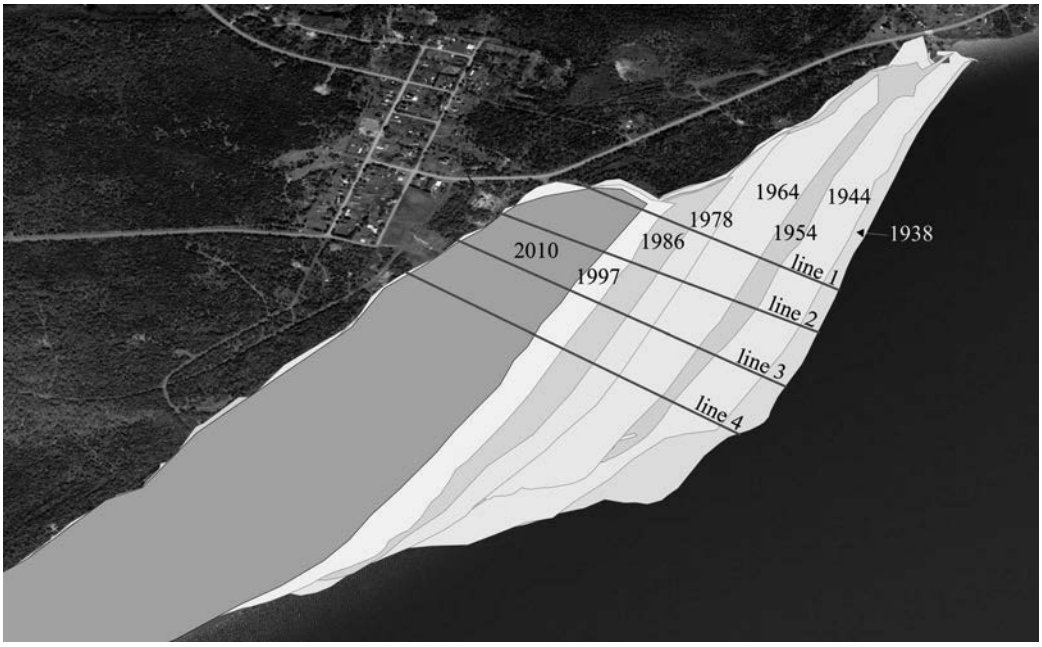

Fig. 5. Four transect lines across Gay tailings pile, showing shoreline erosion down to 2010 condition. Eroded margins are shaded and dated.

on the mode, rather than on the mean. A final estimate came from estimating shoreline regression, i.e., meters of erosion at the shoreline through time for four transect lines (Fig. 5) across the Gay pile, extrapolated to intercept the natural shoreline.

Bathymetric LiDAR and multispectral data—A 1906 bathymetry map (Lake Superior Coast Chart No. 4, Soundings 1906) provided depths at some sites and an estimate of nearshore contours. Although crude, the depth records allowed estimates of underwater shoreline contours before stamp sand encroachment. Bottom contours of the 1906 map were superimposed on the 2008 LiDAR above-ground aerial map of the shoreline stamp sands to more precisely calculate total shoreline volume of stamp sands south of the main pile.

LiDAR imagery was complemented with simultaneously collected MSS imagery on the CHARTS airborne platform. The CASI hyperspectral scanner was configured to acquire data over eight bands uniformly spaced between 375 and 1050 nm, including five visible wavelengths (nominal bandwidth of 84 nm). For distinguishing bay sediments, wavelength studies required the ability to penetrate water and sufficient spectral differences to separate stamp sands from background Jacobsville Sandstone and natural beach sands (Fig. 3a,b). Our main focus was on the green and red portion of the visible spectrum—495–750 nm (Fig. 4a). Delineation of the land–water boundary was best when using near-infrared bands. Additional images of Grand Traverse Bay were retrieved from the National Agriculture Imagery Program (NAIP) multiresolution seamless image databank (years 2005 and 2009).

LiDAR substrate mapping and upwelling multispectral color data helped resolve substrate features and aided distinguishing stamp sands from natural substrates. Concurrent with overflights, we measured water column and sediment characteristics using Michigan Tech's 11.3-m R/V *Agassiz* and 7.3-m R/V *Polar*. Ground-truth Ponar samples clarified the nature of the various substrates in the bay. Samples were photographed and supplemented by underwater video images of sediment surfaces, taken by a MarCum VS620 Underwater Viewing System. Previous underwater images were also available from NWRI surveys (Biberhofer and Procopec 2008).

Interpretation of 8-band 2008 MSS and 2009 3-band aerial photo images was aided by substrate differences in spectral reflectance. As is evident on aerial photo images (Fig. 2), the gray to black stamp sands (crushed basalt) on the beach have a low albedo, whereas the natural white beach sands (derived from Jacobsville Sandstone) have a high albedo. Spectral reflectance of stamp sands, natural beach sands, and Jacobsville Sandstone (coastal rock outcrop) was quantified above and underwater (Fig. 3a,b). Procedures followed Sabol et al. (2008), using an Analytical Spectral Devices (ASD), FieldSpec Pro (model FSP350-2500PJ). Beach substrates included: (1) stamp sands from the primary discharge pile; (2) wave-reworked stamp sands; (3) native beach sands, derived from Jacobsville Sandstone; (4) Jacobsville sandstone; and (5) various mixed stamp sands and natural sands.

Using Lyzenga's techniques to help classify CHARTS MSS substrate types—To quantify downwelling and upwelling spectral irradiance in Grand Traverse Bay, we used a Satlantic OC P1000 Optical Profiling Radiometer at seven sites (Fig. 4a). During the week of 23 June 2008, and during the summers of 2009–2010, additional ground- and sea-truth data were collected. Determining depth limitations

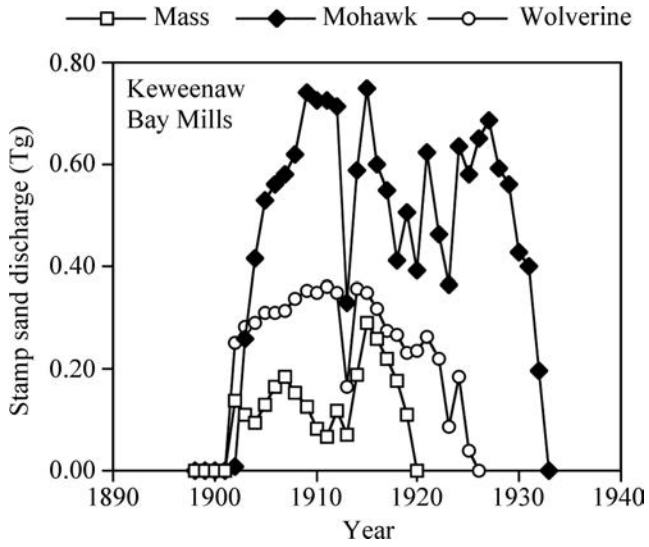

Fig. 6. Yearly stamp sand discharges from large Keweenaw Bay copper mills (Mass, Mohawk, and Wolverine). Mohawk and Wolverine Mills were located at Gay, whereas the smaller Mass Mill was south, near Assinins, north of Baraga. Total stamp sands discharged were Mass 2.7 Tg, Mohawk 16.2 Tg, and Wolverine 6.5 Tg (*see* Table 1).

on the MSS data required three components. The first component was a finished bathymetry map of Grand Traverse Bay, derived from the 2008 LiDAR studies. The second component was a finished MSS mosaic, stitched together from the various overflight tracks. The third component involved calculations from Satlantic spectral radiometer light profiles to help identify upwelling reflectance types and to facilitate substrate classifications.

How deep could MSS resolve bottom sediment details? The Satlantic provided attenuation coefficients for downwelling and upwelling spectral bands (Fig. 4a). Critical additional variables were surface irradiance energy and coefficients for depth-dependent spectral transmission. From these two parameters, we calculated the maximum water depth that light can penetrate, according to the simple formula: $I_z = I_o e^{-\epsilon z}$, where I_z is irradiance at depth z, I_o is surface irradiance, and $-\epsilon$ is the extinction coefficient. However, for MSS resolution, ambient light must reflect off the bottom surface and return a signal to the surface plane, hence the importance of the Satlantic upwelling irradiance measurements. ArcMap software package (version 9.3) was used to create a depth-dependent mask that was superimposed upon the MSS data to check the ability to resolve substrate color contrasts (Jensen 2004).

Lyzenga (1981) provided a method for handling reflectance depth effects in MSS imagery, allowing production of a water depth-independent mosaic:

$$R_w = (A_d - R_\infty)e^{-gz} + R_\infty$$

where R_w is the water column reflectance if the water were optically deep, A_d is the bottom albedo, z is the depth, and g is a function of the diffuse attenuation coefficients for both downwelling and upwelling light.

Table 2. Mass of stamp sands left on the original Gay tailings pile through time.

Year	Mass (Tg)
1938	15.76
1944	14.00
1954	10.72
1964	9.58
1978	7.03
1986	5.63
1997	4.08
2008	3.29

Ratio-based algorithms determine the relation between different spectral bands over the same bottom type. The polygons were then classified by substrate type. By applying this method, we were able to separate different bottom types based on their reflectance. The MSS images were projected to Universal Transverse Mercator Zone 16 coordinate system and pixel values converted to actual spectral reflectance values (W m^{-2}) for comparison with Satlantic data. ArcGIS or ERDAS (Earth Resources Data Analysis System) IMAGINE was used to translate data from MSS images.

Although we had a clear path to follow in classifying different bottom types, there were some typical technical problems with flyover images. These problems were due to different sun angles, cloud cover, and sun glints off waves during the 2-d operations, and sometimes to miscalibrated sensors (data gaps). A simple glint-removal algorithm was applied to the 2008 overflight bands to correct for sun glint artifacts (Hedley et al. 2005). We obtained another 3-band MSS data from an aerial overflight (2009 USDA; http://datagateway.nrcs.usda.gov/GDGOrder.aspx) from calmer lake surface conditions to complement the 2008 set. The imagery was obtained from NAIP. Depth-corrected radiance images were produced for each of the visible bands per image strip. Through visible inspection, bands 2 (490 nm, blue) and 3 (581 nm, green) were chosen as optimal channels for bottom type discrimination. We utilized bottom type's attributes (albedo, color, and depth-corrected radiance) to aid classification, and cross-correlated with sites of actual Ponar substrate samples (ground truth). Depth-corrected images were input into the depth-invariant index algorithm (Lyzenga 1981) to produce one combined bottom type image. Level slicing of the derived depth-invariant bottom type image created a bottom type classification map. The method appeared to clearly differentiate three different shallow-water substrate types: stamp sands, native yellow sands, and Jacobsville Sandstone (bedrock, cobble).

Results

General features—Grand Traverse Bay landforms are shown in Fig. 2 (2005 NAIP, Multiresolution Seamless Image Database–MrSID format, 1-m-resolution image). The bay includes about 8.5 km of shoreline where dark stamp sands lie over formerly white native beachfront

Fig. 7. (a) Wave erosion of the Gay tailings pile. The near-vertical 7-m bluffs contain well-preserved remnants of wooden troughs that sluiced stamp sands across the pile. (b) Primary and secondary sluiceways (Wolverine Mill, winter 1922) carry stamp sands over the Gay pile. Lake Superior is on the horizon. Notice melted regions with fresh discharges. Photo courtesy of Michigan Tech Archive.

derived from Jacobsville Sandstone. Eroding dark sands have covered around 2.3 km^2 of beach surface over the last 70 yr. The northernmost thousand meters of coastline contain the original tailings pile, an area that appears slightly purple from the Fe-oxidized slime clay fraction, and reaching $>$ 6–7-m elevation above water. The pile shoreline features a weathered bluff fronted by a narrow sinusoidal beach (Fig. 7a). The beach varies from 5 to 8 m wide. South of the pile, the redeposited stamp sand portion is fairly level and ranges from 45 to 530 m in width, with numerous small ponds. There is residential housing along $\sim$ 1,125 m of shoreline north of the Traverse River harbor. Immediately south of the harbor break-wall, the shoreline is also residential with typical white sand beach from weathered Jacobsville Sandstone.

The aerial photo (Fig. 2) reveals long stretches of stamp sands along the middle beach region that penetrate into the forest margin and wetland edges. About 1.5 km north of the Gay pile is the Tobacco River, which marks the northern drift of stamp sands, whereas 6.9 km south in the bay is the Traverse River, where dark stamp stands stop abruptly, abutting up against an extended Army Corps seawall. In between, in the middle of the bay, stamp sands have mounded up south of the pile and around the Coal Dock site, forming a small pond behind the dock. At present, an unnamed intermittent stream floods the pond in early spring and exits through the stamp sand beach margin. Small remnants of the original white beach sands show up behind the Coal Dock and in an elevated fringe north of the Traverse River seawall. Inland there are about 60 alternating post-Pleistocene (Nipissing) beach ridges distinguished by different vegetation types, switching between pines (*Pinus*) and spruce (*Picea*) on upland highs and grasses in lowland swales. The Nippising beach ridge complex demonstrates that the southern portion of the bay is a region where eroded sediments were deposited as beach sands for 3800–900 yr before present (B.P.) during dropping lake levels. Dated cores suggest that a beach ridge formed every 36 $\pm$ 7.8 yr, and that the strandline progradation rate was 0.68 $\pm$ $-$0.1 m yr^{-1} (Johnston et al. 2000). South of the

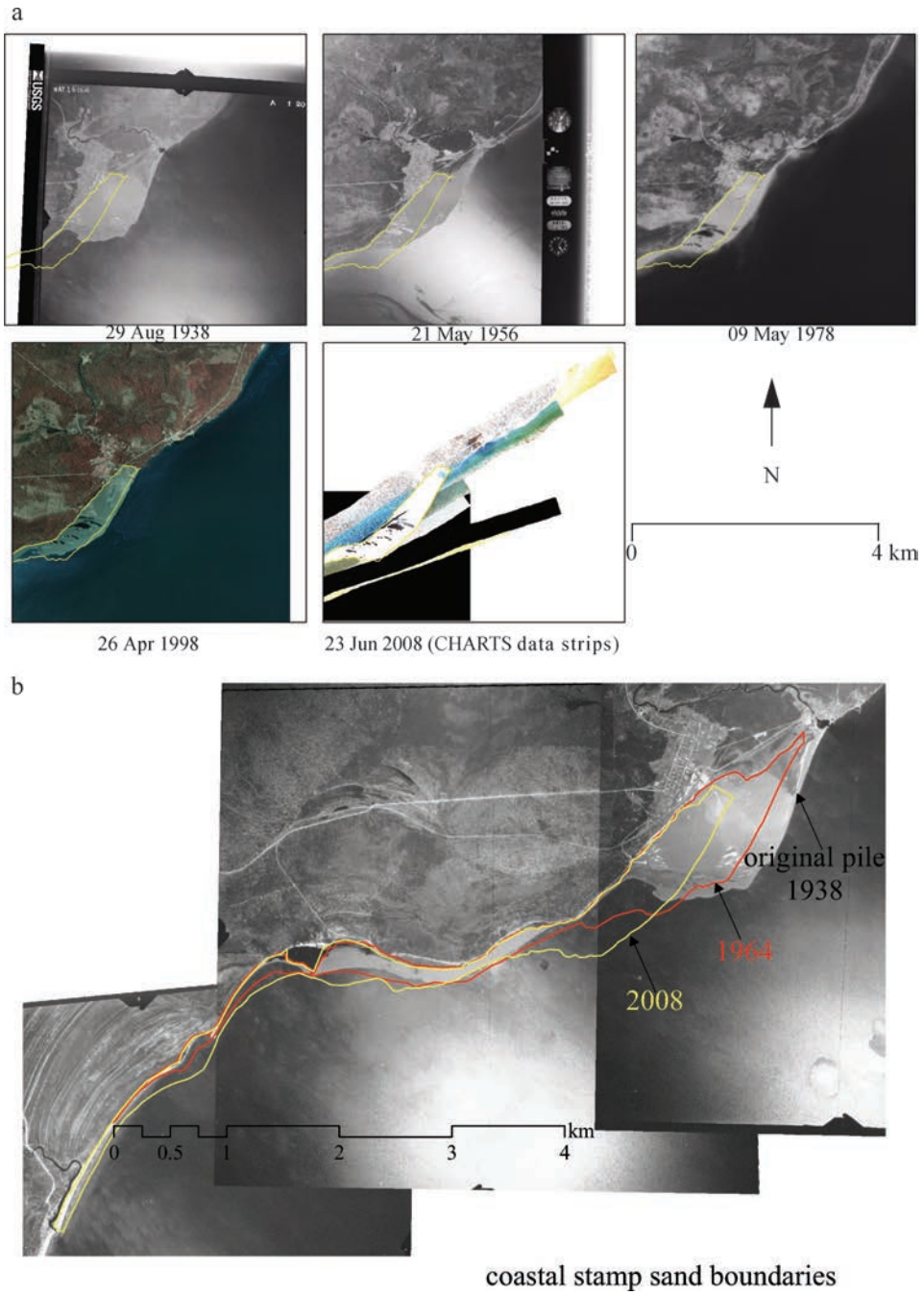

Fig. 8. Selected aerial photos record erosion of the Gay tailings pile: (a) LiDAR-derived outline of 2008 pile superimposed upon various aerial images; (b) changing boundaries of coastal stamp sands indicated on original 1938 aerial image (red—1964 outline; yellow—2008). Note the diminished original tailings pile and the greater spread southward of stamp sands as time progresses.

Traverse River seawall, relatively undisturbed white beach sands stretch for another 5 km.

Historic mill discharges and Gay tailings pile—Company records document that the Mohawk and Wolverine companies mined the Kearsarge amygdaloidal basalt deposit and constructed new stamp mills at Gay during the summers of 1901–1902. The two operated as twin mills, with a single pumping plant and a joint superintendent. Stamp rock was hauled from the mines to the stamping site via the Mohawk and Traverse Bay Branch (Mineral Range Railroad), a distance of about 21–27 km (Monette 1992). Coal for operations was unloaded south of Gay, requiring construction of a Coal Dock (Fig. 2), and laying of a short

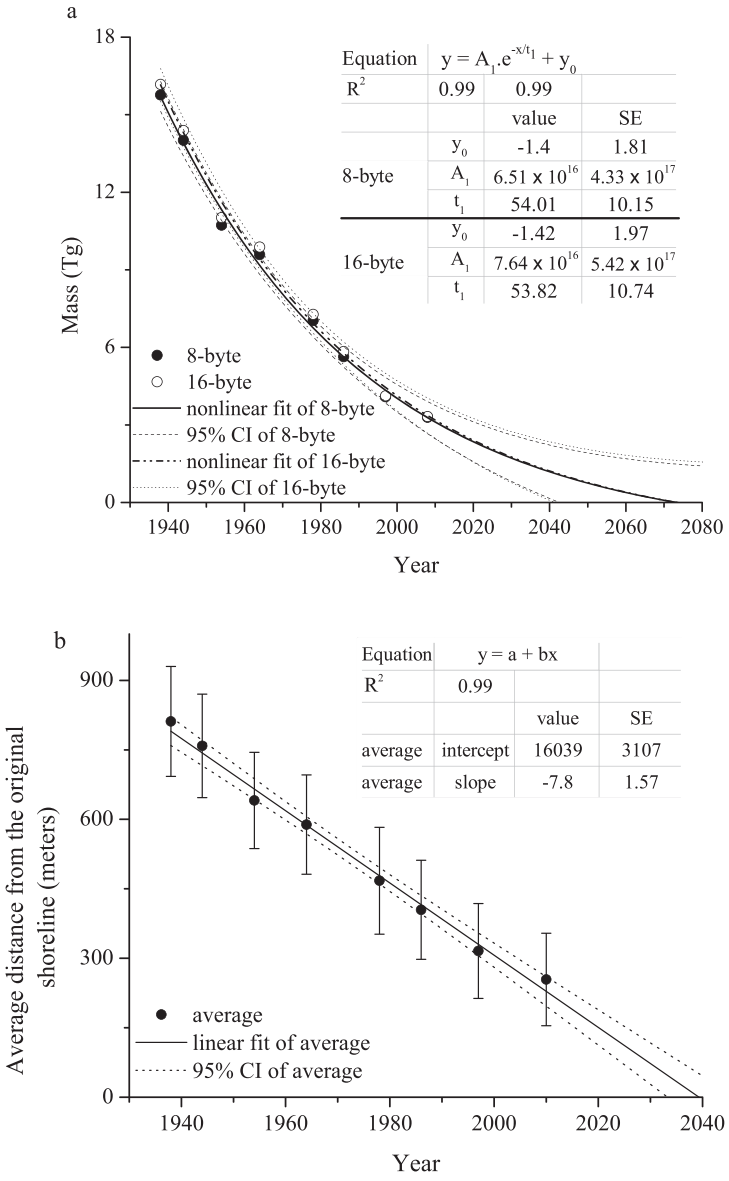

Fig. 9. Erosion of mass from the primary tailings pile: (a) loss of mass in teragrams from the Gay tailings pile through time is an exponential decay function (8- and 16-byte equations converge, Table 3), with a zero intercept around 2074; (b) in contrast, shoreline erosion in meters appears nearly linear, with a mean intercept around 2040 (Table 3).

connecting line. The Coal Dock extended 100 m into the bay, 5.7 m deep at its end (Clarke 1978).

Three major mills discharged into Keweenaw Bay (Fig. 6; Table 1). The Mohawk and Wolverine Mills were located at Gay, whereas the Mass Mill was to the south near Assinins, north of Baraga. Operations at the Mohawk and Wolverine Mills were much larger than at the Mass Mill. The beginning of Keweenaw Bay stamp mill operations was nearly synchronous, as the Mohawk (1901), Wolverine (1902), and Mass (1902) Mills opened within 3 yr of each other and closed between 1919 and 1932 (the dates were Wolverine 1925, Mohawk 1932, Mass 1919; Butler and Burbank 1929; Kerfoot et al. 2009). The Mohawk and Wolverine Mills utilized Nordberg stamps, Harding ball, and Chilean mills. The two stamp mills sluiced a combined 22.7 Tg of stamp sands onto one large pile, covering about 0.9 km^2 originally (Figs. 5, 8). By 1915–1920 a water intake tunnel extended out a distance of 856 m and a stamp sand conveyor belt 527 m into Grand Traverse Bay (Monette 1992). As a cross-check on discharge, our estimated total discharge at Gay (i.e., 22.7 Tg) corresponds closely to the total of 21.8 Tg reported by Babcock and Spiroff (unpubl.).

Erosion studies using LiDAR and aerial photographs—From a combination of the 2008 LiDAR bathymetry profiles and several aerial photographs (Fig. 8), we estimated the mass of stamp sand eroded from the pile through time, and the portion left along the shoreline site

Table 3. Regression equations for erosion of the Gay tailings pile (time is x, as the year, e.g., 1998). Equation variables and constants, including R^2 values, x-intercept (date of zero stamp sand mass), and 95% confidence limits for dates around the zero mass intercept are given. Nonlinear mass erosion equations are included below, whereas $\log_{10}$-transformed version is the last entry under linear.

Linear						
No.	Source	Slope	R^2	x-intercept	Lower limit	Upper limit
1	Distance line 1	−7.6	0.99	2021	2016	2026
2	Distance line 2	−7.9	0.99	2039	2033	2046
3	Distance line 3	−8.0	0.99	2044	2037	2052
4	Distance line 4	−7.9	0.99	2050	2043	2059
5	Average distance	−7.8	0.99	2038	2033	2046
6	$\log_{10}$ of mass+1 (linear fit)	−0.019	0.99	2082	2077	2091

Nonlinear								
Equation	Source	y_0	A_1	t_1	R^2	x-intercept	Lower limit	Upper limit
$y=A_1\times e^{(-x/t1)}+y_0$	8-byte nonlinear	−1.42	6.51×10^{16}	54.01	0.99	2073	2042	>2080
$y=A_1\times e^{(-x/t1)}+y_0$	16-byte nonlinear	−1.42	7.64×10^{16}	53.82	0.99	2073	2041	>2080

(*see* Methods; Table 2). Graphing the values, the time course for mass lost through time from the original tailings pile was clearly nonlinear (Fig. 9a). The best fit was obtained with an exponential decay function (Table 3, $y = 7.646 \times 10^{16} e^{-x/53.82} - 1.42$, where x is in calendar years; $R^2 = 0.993$). With the exponential decay model, the zero intercept (indicating when the pile will be gone) was around 2073. The 95% confidence intervals fit around the nonlinear regression trend indicate uncertainty in decades (Table 3; 2041 to > 2080). Of the 22.8 Tg stamped and discharged by the Mohawk and Wolverine Mills (Table 1), an estimated 15.8 Tg (69.3%) remained on the Gay tailings pile in 1938. Estimating mass erosion through time (Table 2), we found that only 3.07 Tg (13.5%) of the original discharged mass was still on the pile in 2008. By 2008, yearly erosion loss was about 42,050 m^3 of stamp sands, or about 0.069 Tg. A second estimate of mass erosion loss came from $\log_{10}$ transformation of volumes (*see* Methods; Table 3). As expected for exponential decay, the $\log_{10}$ transformation allowed a linear fit to the data points (Table 3; $n = 8$; $y = -0.01978x + 41.1879$; $R^2 = 0.993$). The linear regression produced a zero intercept of 2082, with 95% confidence intervals of 2077–2091.

A third way of estimating erosion from the Gay pile was to calculate meters of shoreline lost each year, using four transect lines across the pile, each at right angles to the shoreline (Fig. 5; Table 3). These measurements, derived from georegistered aerial photographs, show that the loss in meters of shoreline each year has remained nearly constant through time (Fig. 9b, $y = -7.86x$, $R^2 = 0.990$), i.e., around 7.9 m yr^{-1}. The four transect lines gave zero estimates between 2021 and 2050 (Table 3). The nearly constant loss of shoreline per year is intriguing. The nonlinear erosion of mass through time is associated with the greater water depth (and stamp sand volume per slice) occupied by stamp sands back in 1938 (5 m) relative to the lesser depth (2 m) occupied today. While the exact mechanism that produced such a nice exponential decay curve is uncertain, deeper waters along the coastline are subject to stronger currents (Keweenaw Current; Chen et al. 2001; Zhu et al. 2001). Another possible contributing factor to a nonlinear mass loss recently is that the northern part of the pile is becoming better shielded behind the natural shoreline (Fig. 2), protecting it against the strong southerly currents during winter storms. The distance that stamp sands have moved along beaches in Grand Traverse Bay is only one-third the distance along the more energetic west coast (from Freda to Redridge, 21 km of movement; whereas from Grand Traverse, the value is about 7.4 km; Kerfoot et al. 2009).

Although pre–mining- and mining-era bathymetry maps are rare for Grand Traverse Bay, depths and contours were obtained from a 1906 map (*see* Methods). Although primitive, the depth contours allowed estimates of stamp sand mass underneath the above-water volume measured by LiDAR (Fig. 10). Once the total volume of stamp sand along the shoreline was estimated, the amount that had eroded into the bay by 2008 was indirectly calculated, essentially by difference. Pixel calculations estimated the mean depth for the entire shoreline (pile + southern redeposited portion) as 2.94 m (SD = 1.07). For the entire shoreline (pile + southern portion), the above-water total mass was estimated from the 2008 LiDAR as 4.53 Tg, whereas the mass under the shoreline edge was estimated using the 1906 contours as 7.15 Tg, giving a total shoreline mass of 11.68 Tg. Both the 2008 above-water thickness on the Gay pile and the complete shoreline stamp sand thickness map are shown in Fig. 10. Two regions of shoreline contain much larger amounts of underwater stamp sands, the Coal Dock region and a secondary region just south of the primary pile. In retrospect, the Coal Dock was constructed in one of the deepest shoreline regions, 5–7 m deep.

A final estimate from the 2008 LiDAR concerned road use of stamp sands. Starting in the 1950s, a certain amount of stamp sand was removed by the Keweenaw Road Commission from the inland side of the Gay pile, for application on roads during winter. However, given the

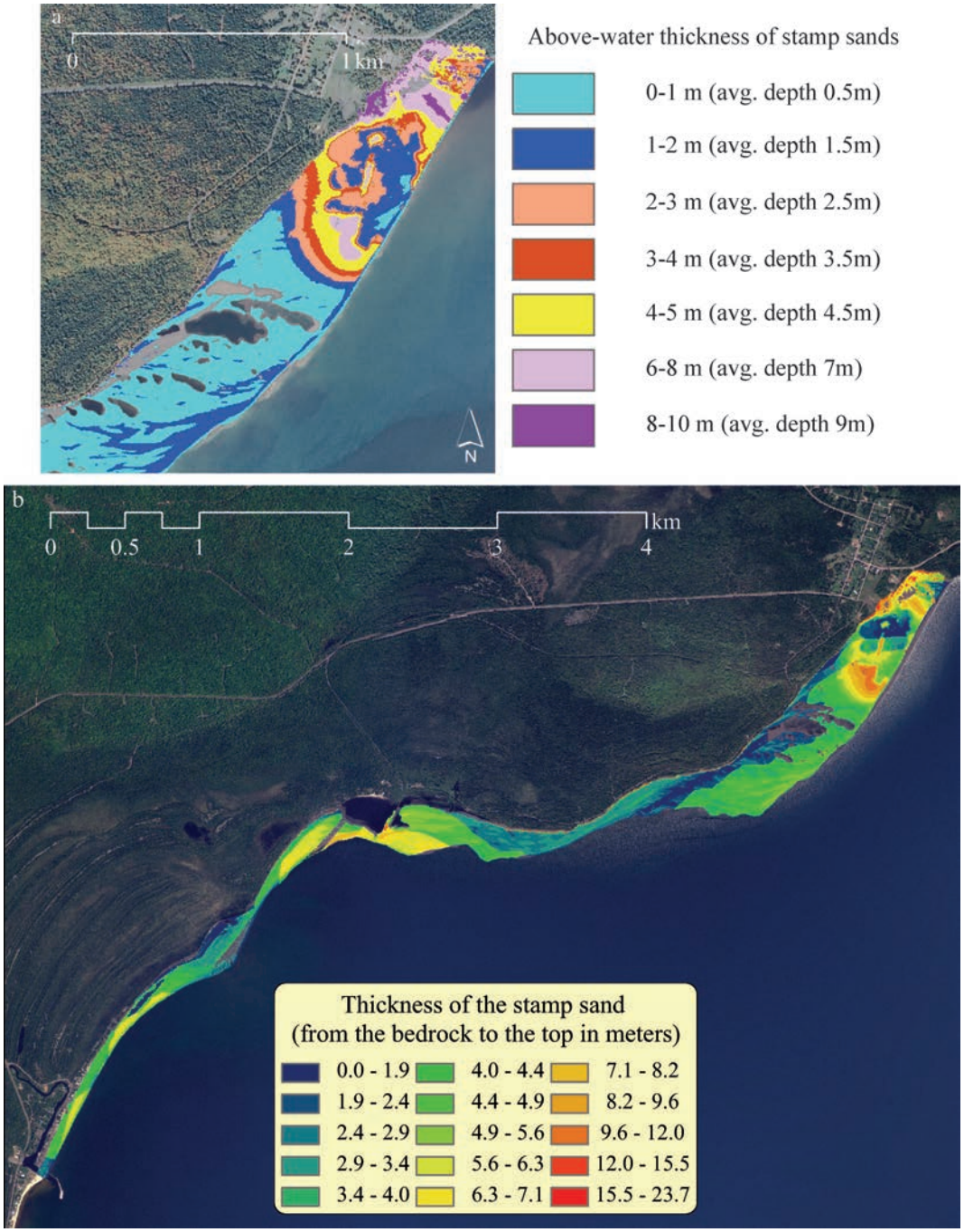

Fig. 10. Thickness of coastal stamp sands: (a) thickness of above-water stamp sand on the main Gay tailings pile (from 2008 LiDAR); (b) total thickness (above + below water) of coastal stamp sands, bedrock to top of above-water portion (2008 LiDAR above-water plus 1906 underwater bathymetry depth). Depths are color coded. The large gray-black objects in redeposited stamp sands south of the Gay pile are a series of ponds.

high resolution of LiDAR and the clear gouges left on the pile by the Road Commission, we could estimate the road application loss as 1.01 Tg of the Gay pile total (4.4%). So of the 22.7 Tg originally discharged onto the pile, 11.68 Tg (51.5%) was redeposited along the shoreline, and 1.01 Tg (4.4%) was removed for road application. By difference, the remaining 10.01 Tg (44.1%) moved into Grand Traverse Bay to spread as an underwater cover (Table 4).

Underwater bottom features—The CHARTS LiDAR images resolved several intriguing underwater features (Fig. 11). Considering the combination of instrument spatial resolution and the low altitude of overflights in this project, the amount of detail in collected images was orders of magnitude higher than that obtained from routine geospatial imagery platforms. LiDAR penetrated 2.5 times deeper than natural light, to 22 m. Progressing southward

Table 4. At the time of the 2008 overflight, estimated mass of stamp sands remaining on pile, redeposited along shoreline south of original pile, and washed into Grand Traverse Bay (by difference).

Stamp sand estimate	Estimated mass	
	Tg	%
Original discharged mass (1901–1932)	22.79	100
Gay pile (total 2008)	3.07	13.5
Shoreline (above portion 2008)	4.53	19.9
Shoreline (below portion 2008)	7.15	31.4
Total shoreline (original pile+redeposited onshore 2008)	11.68	51.5
In Keweenaw Bay (difference)	10.01	44.0

from offshore of the Gay tailings pile, we found: (1) a bedrock shelf escarpment of Jacobsville Sandstone with long stamp underwater ''sand dunes'' parallel to shore; (2) a submersed trough, which seemed to be an ancient riverbed, east of the Buffalo Reef region; (3) the raised promontory of bedrock and cobbles that form Buffalo Reef; and finally (4) a relatively low-gradient underwater sandy terrain south of the Traverse River that ended in a series of small ''comblike'' eastward-directed channels. Toward the north, immediately south of the Tobacco River, the coast seemed mostly an erosion environment, with steep bedrock scarps and migrating underwater ''dunes'' of stamp sands, whereas toward the south, past the Coal Dock, it seemed a depositional environment. In the southern region, the redeposited stamp sands formed recent additions onto the series of Nipissing beach ridges.

In the middle of Grand Traverse Bay, Buffalo Reef is composed of two separate rises, slightly displaced from each other (eastern promontory is shifted northward). A deep cleft (underwater canyon) runs through the structure. The displacement in the two underwater ridges suggests an

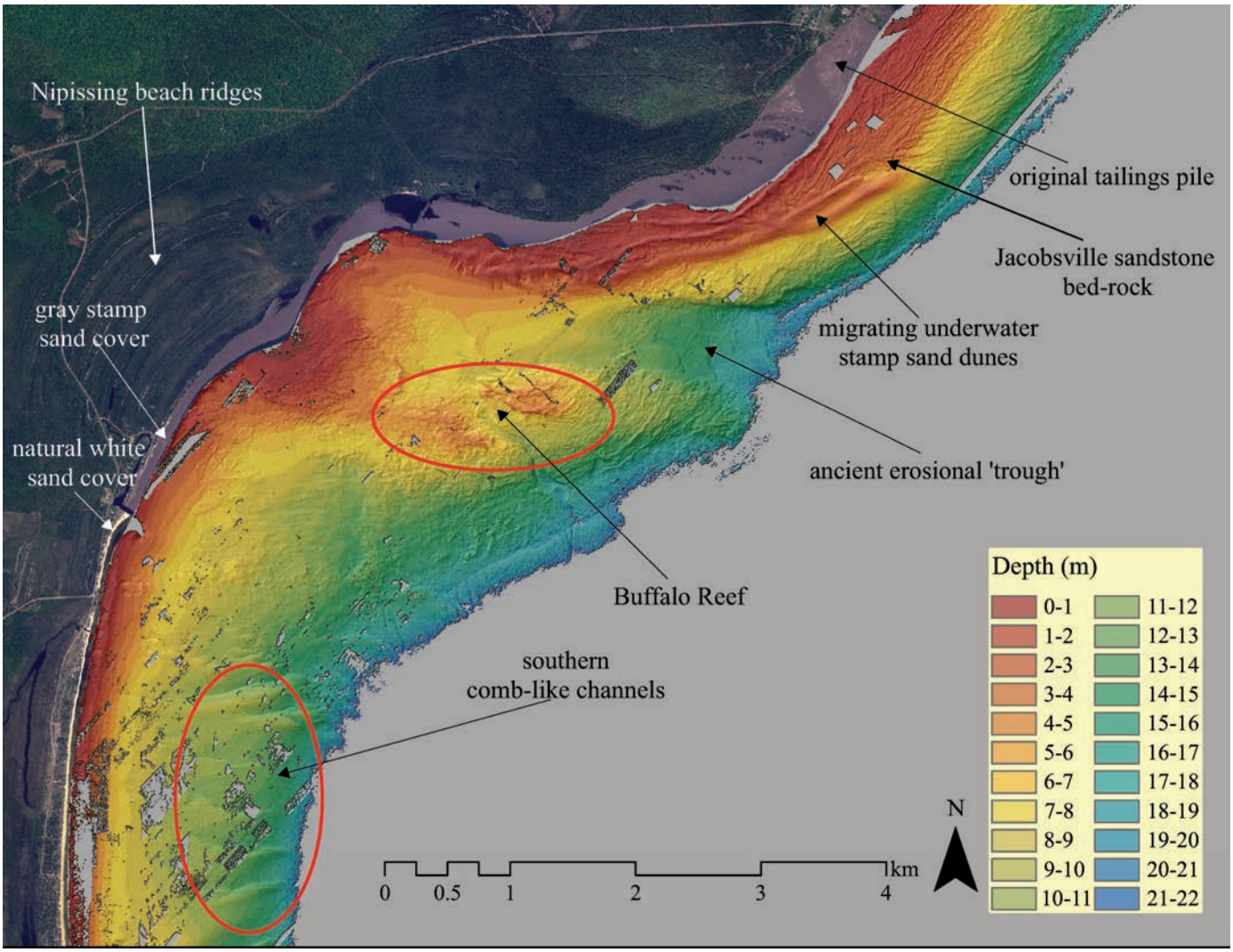

Fig. 11. Contour-colored LiDAR bathymetry of Grand Traverse Bay juxtaposed against terrestrial aerial photo image (2005 NAIP). LiDAR reveals several prominent bottom features (Jacobsville bedrock, migrating ''dunes'' of stamp sand, ancient river ''trough,'' the twin promontories of Buffalo Reef split by a cleft, and the southern ''comblike'' channels), whereas MSS highlights the terrestrial Nipissing beach ridges. Irregular black patches on substrate contours are no-data regions.

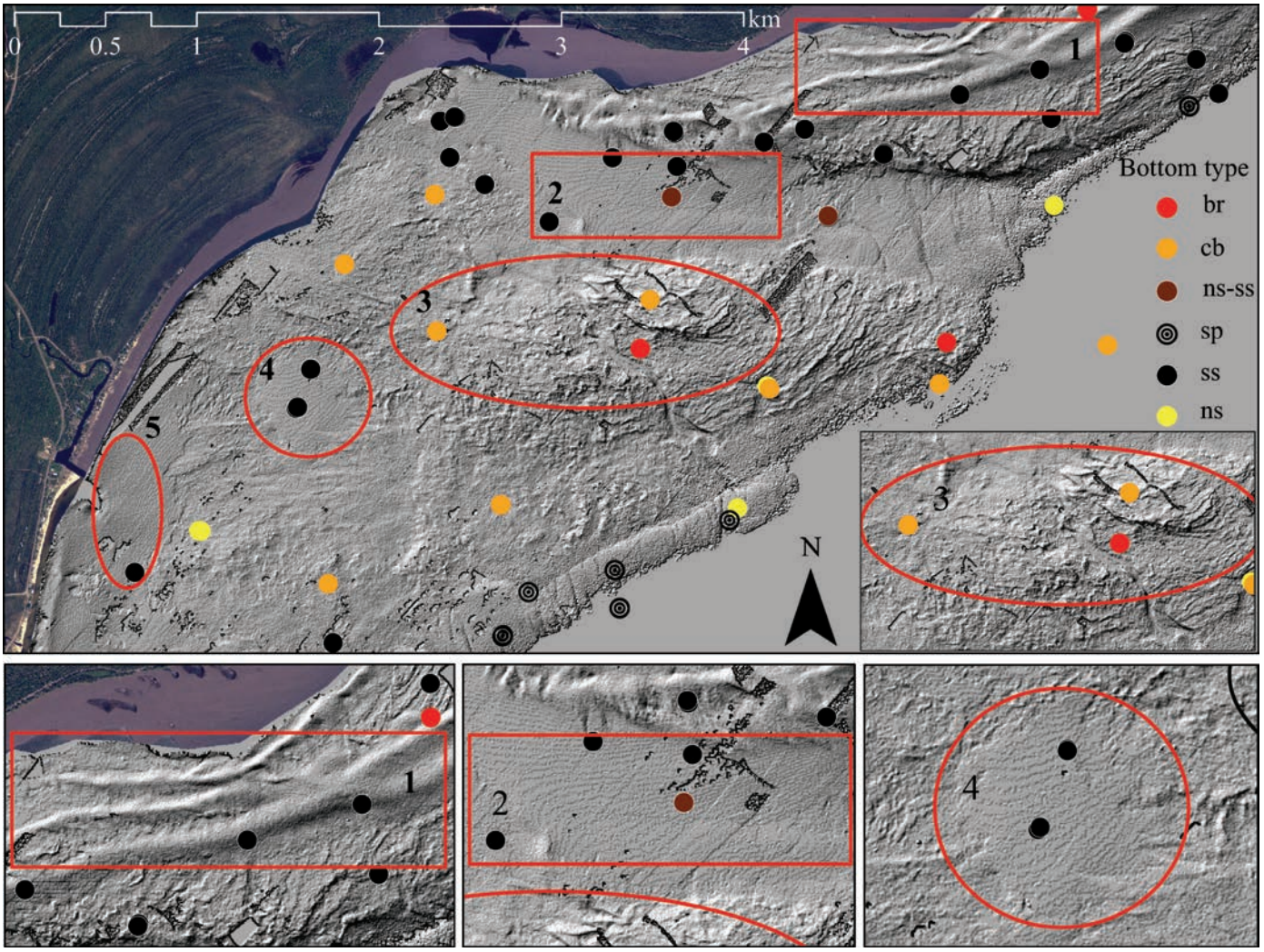

Fig. 12. "Hill shade" technique highlights bathymetric structures. Note the funneling of underwater stamp sand "dunes" (No. 1 inset) into the upper regions of the "trough" north of Buffalo Reef. The western upper trough stretches are covered by stamp sands and appear smooth (No. 2 inset) in contrast to the lower reaches that resemble riverbed eroded Jacobsville Sandstone. On Buffalo Reef (No. 3), regions of bedrock and cobbles are evident as coarse bottom irregularities. Other topographic lows to the west of Buffalo Reef (No. 4, No. 5) also seem filled with stamp sands. Ground-truth sample sites indicate red (br, bedrock), orange (cb, cobble), deep brown (ns-ss), gray (sp, salt and pepper), black (ss, stamp sand), red yellow (ns, natural sand).

old fault, subsequently eroded into a narrow canyon between the two peaks at the same time that the river channel (trough) was eroded. The erosion happened before Buffalo Reef became submersed more recently along the coast. The underwater canyon and trough suggest low water levels in Lake Superior thousands of years ago.

In Fig. 12, a "hill shade" technique (ArcMap 9.3, Spatial Analyst; Jensen 2004) has been applied to highlight underwater benthic surfaces on the LiDAR map. There are several regions in this figure that have intriguing characteristics. The area in rectangle No. 1 reveals underwater stamp sand "dunes" migrating south- and westward. Ground-truth sampling (black dots) confirmed that these "dunes" were composed of coarse stamp sands. The "dunes" appear to stretch out until they reach the northern portion of the trough, off the Coal Dock. One could interpret the structures as ribbons of coarse sand transported via strong wave action and powerful coastal currents across bedrock to the trough edge, where they spill over into the upper and middle reaches. The trough (rectangle No. 2) seems a 3-km-long structure, scoured to a depth of 2 m below surrounding bedrock. The lower reaches of the trough appear to be bedrock, as eroded bedding planes of Jacobsville Sandstone cut across the surface. Recognition of the trough now explains why the Coal Dock region was anomalously deep, i.e., it coincided with the upper reaches of an old eroded river channel. It is possible that the Coal Dock effectively served as a groin during erosion of the main pile, deflecting migrating stamp sands into the upper reaches of the trough.

Buffalo Reef is elevated above the local coastal margin slope, with topographic irregularities suggesting bedrock and coarse cobble. The reef seems weathered by wave action out of Jacobsville Sandstone into a southeastward-directed promontory. The underwater trough (Figs. 11, 12) lies to the immediate northeast. The upper reaches of the trough surface texture seem unusually smooth, suggesting

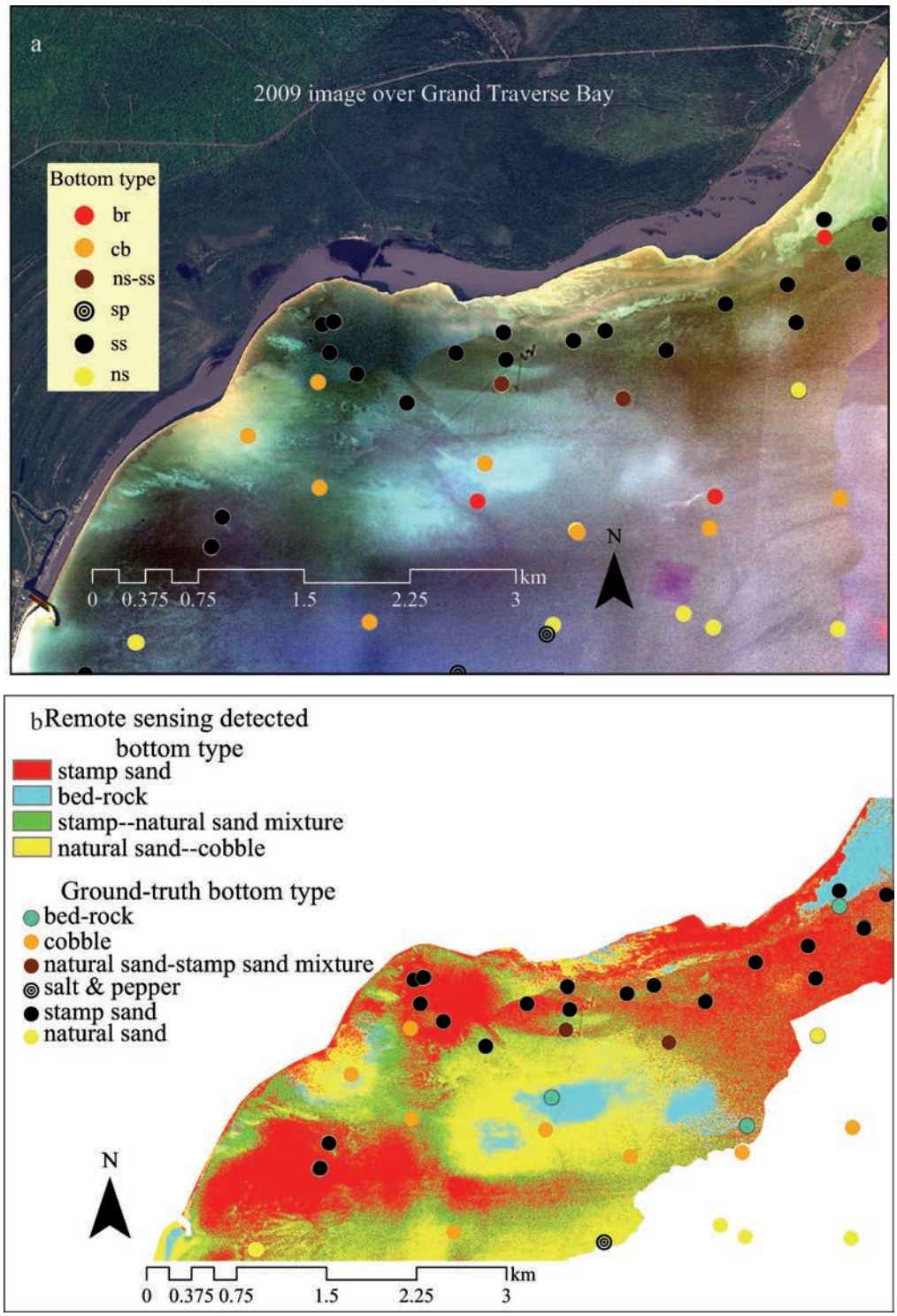

Fig. 13. (a) A processed 3-band (2009 USDA) image of nearshore Grand Traverse Bay, and (b) the subsequent substrate classification. The 3-band image contrasts bottom coverage by high-albedo bedrock and cobble regions (blue, yellow) with low-albedo stamp sand cover (red). Ground-truth benthic ship samples are color-coded circles (bedrock, cobble, natural sand mixed with stamp sands, salt and pepper, stamp sand, natural sand).

stamp sand filling (rectangle No. 2). Filling was verified by Ponar sampling. At the middle of the trough, there is a mixture of stamp sand and natural sand (brown dots, Fig. 12). Thus, the LiDAR map suggests that nearly half of the trough's bottom is covered by stamp sand. Shipboard Ponar sampling also indicates size sorting of stamp sand and natural sand in the upper and middle reaches of the trough. Stamp sand near the shoreline is coarse grained, resembling above-water coastal sand, whereas deeper samples contain much more silt and clay. This attribute is

expected from wave energy gradients, as finer material will settle in the deeper, lower-energy regions.

Toward deeper coastal regions, we find salt-and-pepper textures in top sediments (Fig. 12). These patterns show a sprinkling of coarse stamp sand particles on top of fine deep-water brown silt and clay mud. The patterns could arise if winter ice carried coarse stamp sands from beaches into deeper waters, where melting released the particles to sprinkle upon the typical finer lake silt-clay sediments. Stamp sand particles increase in top sediments, a pattern expected if the stamp sand source is getting closer, as stamp sands migrate down the coast.

MSS classification: stamp sand moves into trough and threatens Buffalo Reef—An analysis of substrate spectra (Fig. 3a,b) reveals that the stamp sands are visibly darker than most of the materials against which they would be juxtaposed in nature. Moreover, significant differences exist between stamp sands and background materials in the high ends of the green portion of the spectrum and especially into the red portion of the spectrum.

Buffalo Reef margins include cobble-covered outlying regions that lead to a Jacobsville Sandstone bedrock promontory of $\sim$ 3.1 km^2, divided by the steep crevice. High-resolution LiDAR showed that the reef has two lobes, a 2.0-km^2 plus a smaller 1.1-km^2 region. North of Buffalo Reef there is an underwater promontory that may also have helped divert stamp sands southward into the trough. Along the promontory, however, there is a low depression where migrating stamp sands may have broken through and moved westward. In polygons No. 4 and No. 5 (Fig. 12), there are closed depressions filled with coarse stamp sand (black dots, sediment sampling sites).

We used a 3-band aerial photo image from a 2009 USDA NAIP overflight to map underwater substrates (*see* Methods). Figure 13 illustrates the depth-compensated color image and the subsequently derived substrate classification map. In the depth-compensated (Lyzenga 1981) image, stamp sands stretch as irregular patches along the shoreline and in front of, and behind, Buffalo Reef (Fig. 13a). Migrating underwater stamp sand dunes show up as orange ribbons parallel to the shoreline, below the Gay pile and western redeposited stretch. Around the Coal Dock, the ribbons spread out to intercept the trough north of Buffalo Reef. Figures 11, 12 also revealed the slight northern ridge that may have deflected westward migrating sands into the trough and through a low-lying ridge. Indeed, low-gradient "flat" bottom can be seen in Fig. 12 (insets No. 4, No. 5), where ground-truth stations confirm stamp sand. In the image, there are also reaches of exposed Jacobsville Sandstone bedrock below the Gay pile, and cobble and bedrock stretching out around Buffalo Reef (Fig. 12).

Buffalo Reef is a productive spawning area for whitefish (*Coregonus clupeaformis*) and lake trout (*Salvelinus namaycush*) potentially threatened by movement of stamp sands (Chiriboga and Mattes 2008). Transgression of moving stamp sands into cobble fields that surround Buffalo Reef is not conducive to normal hatching of fish eggs, for the sands may fill crevices or may be toxic for eggs or newly hatched larvae (Chiriboga and Mattes 2008). An enlargement of the trough illustrates relatively smooth sands extending down halfway along the slope, forming small ripples along the surface (Fig. 12; inset No. 2). Below the halfway point, there are bedding features of Jacobsville Sandstone that suggest eroded hard rock substrates. Based on our substrate map, tribal concerns are fully justified, as stamp sand appears to have encircled three-fourths of Buffalo Reef (Fig. 13b).

Discussion

Evaluation of LiDAR and MSS data—One aim of this study was to evaluate the effectiveness of the airborne CHARTS sensor system for generating environmentally useful information for coastal zones of large lakes. Working with aerial photography, the above-water LiDAR mapping allowed us to reconstruct erosion of the original tailings pile and to quantify the fate of migrating stamp sand. Bathymetric LiDAR maps (Figs. 11, 12) revealed intriguing geomorphic structures and processes occurring along the coastal shelf, e.g., ancient riverbeds and fault scarps. LiDAR bottom reflectance also provided single-band information on irregular to smooth bottom types (wave-form measure of "rugosity," not discussed here). The substrate classification corresponded closely with independent sonar and underwater video substrate maps done by NWRI (Biberhofer and Procopec 2008). However, for the first time, the extent of stamp sand underwater cover could be determined.

The CASI 1500 is a hyperspectral scanner that was used here in a multispectral mode (MSS 8-band; i.e., broad-band). Justification for this approach is evident in the ASD hyperspectral reflectance measurements of retrieved submersed sediments (Fig. 3a,b). Signatures of above- and below-water sediments exhibited broad spectral differences without the distinct spectral peaks commonly evident in terrestrial vegetation studies. The broad spectral bands used further served to provide more integrated energy in the measured signal, increasing the signal-to-noise ratio and likely achieving greater depth penetration. Bottom classifications resulting from MSS, CASI, and bathymetric LiDAR showed good agreement with submersed sediment samples retrieved as part of the ground-truth effort. We must note, however, that some spatial difficulties were encountered immediately off the mouths of the Tobacco and Traverse waters, where exiting humic-stained waters created false-bottom readings.

We also need to point out that an airborne scanner imaging system does not represent an instantaneous or synoptic view of the overflight area. The sensor may take hours, or even days, to fly the adjoining flight lines. Different tracts along the scan line will have different bidirectional reflectance angles relative to the sun, resulting in sun glint commonly occurring in certain parts of the scan. Over the time of the overflight, cloud and wind (sea state) conditions may change and water level may also change (in seiche or tidally influenced areas). These artifacts require significant effort to remove and correct. This study also incorporated a significant level of ground-

truth data collection to characterize bottom and water column optical properties. One could ask if the extra effort is worthwhile relative to truly synoptic imagery obtainable from satellites. The answer probably is investigation specific, whether enhanced detail is necessary to reveal important properties or to allow precise calculations.

Ecosystem effects—This study revealed that the time course of events associated with unmitigated legacy mining caused progressive environmental effects that continued for over a century and to this day. As wave erosion of the original pile proceeded, the coarse fraction was moved from the original 0.9-km^2 deposition cone southward as a sorted black sand lens to cover an estimated 1.3 km^2 of white Jacobsville Sandstone beach sands (Weston 2007) and to spread over 5.1 km^2 of bay bottom sediments. Our estimate of 1.3-km^2 shoreline beach stamp sands is less than the 2.3-km^2 estimate of Rasmussen et al. (2002) because the latter calculation used the discredited geographic coordinate reference system for area measurements. So over the 110 yr since discharge, the total surface area of shoreline covered by stamp sands increased 178% (original pile now 0.3 km^2, beach sands 1.3 km^2 = 1.6 km^2), whereas the underwater surface area of bay bottom sediments covered by submersed sands increased 567%. Stamp sands have now moved 7.4–8.1 km south from Gay, extending to the northern seawall of the Traverse River, where they affect the beachfront community.

Ecosystem effects are not restricted to wave-propagated movement of the coarse fraction (stamp sands). In winter, drifting pack ice may incorporate coastal stamp sands and accelerate movement of stamp sand constituents along beaches or across the shelf (Budd et al. 1999). Sediment trap studies of dispersing "slime clay" fractions from the Freda–Redridge stamp sands, off the western coast of the Keweenaw Peninsula, found copper (Cu) concentrations between 50 and 2,000 μg g^{-1} with elevated Cu concentrations (100–340 μg g^{-1}) 20–80 km down-current from the discharge site (Urban et al. 2004). Serious dispersal is also occurring in Keweenaw Bay, as stamp sands move along the beach. Clay-sized particles winnow out of the original tailings pile or from ground-up sands, and disperse widely across bay waters. The clay-sized particles move southward via long-shore currents, ending up in deep-water Keweenaw sediments and in the mid-bay Keweenaw Trough. The enhanced Cu concentrations appear in sediment core profiles (Fig. 1; Kerfoot et al. 1994, 2004; Gewurtz et al. 2008). The long-distance movement of the slime clay fraction explains high correlations between mining-associated metals (Cu, Ag, Hg) in Keweenaw deep-water sediment profiles (Kerfoot et al. 2004). A deep-water NOAA sediment core kilometers off Gay recorded buried maxima over 330 μg g^{-1}, relaxing back to 220 μg g^{-1} in surface strata (Kerfoot et al. 1999), both above state probable effects concentration levels (149 μg g^{-1}).

Potential environmental effects of stamp sands in Grand Traverse Bay are expected to be high. Previous knowledge is available on the elemental composition and toxicity of stamp sands. In stamp sands, Cu occurs at toxic levels for aquatic systems and there is a secondary suite of metals (Ag, As, Cd, Co, Cr, Hg, Mn, Ni, Pb, Zn) that often flag aquatic protection levels (Malueg et al. 1984; MDEQ 2006; Kerfoot et al. 2009). Stamp sand concentrations of Cu are high, averaging 10 to 100 times greater than other regional source materials or natural sediments, with elevated Cu : Zn ratios (Kerfoot and Robbins 1999; Jeong and McDowell 2003). Slime clay fractions (< 1 μm) also tend to be enriched in metals (Cu 2.8×, Zn 3.4×, As 1.3×) above coarse fractions, due to higher surface : volume ratios plus an absorbing rime of Fe and Mg (Kerfoot and Robbins 1999).

Our estimates of stamp sands discharged into Keweenaw Bay from three major mills (Mass, Mohawk, Wolverine; Table 1) are 25.8 Tg. Stamp sands from Gay have been characterized by several methods, including atomic absorption (Jeong et al. 1999); neutron activation (Kerfoot and Robbins 1999), and inductively coupled plasma mass spectrometry (MDEQ 2006, Kerfoot et al. 2009). Early studies of Cu concentrations in Gay coarse stamp sand found values ranging between 1620 and 5486 μg g^{-1} (mean 2697 μg g^{-1}, $n = 7$; Kerfoot et al. 2002, 2009), whereas more recent sampling studies by the Michigan Department of Environmental Quality (MDEQ) on the Gay tailings pile found Cu concentrations 1500–13,000 μg g^{-1} (mean 2863 μg g^{-1}; $n = 274$) and only slightly lower, 710–5300 μg g^{-1} (mean = 1443 μg g^{-1}; $n = 24$) for the southern redeposited beach sands (MDEQ 2006). Metals in the secondary suite at the main Gay pile averaged concentrations of Ag 0.4–7.7 μg g^{-1} (mean 1.8), As 1.0–15.5 μg g^{-1} (mean 1.5), Cr 18–52 μg g^{-1} (mean 28.8), Co 16–36 μg g^{-1} (mean 22.9), Hg 0.06–0.11 μg g^{-1} (mean 0.027), Ni 20–48 μg g^{-1} (mean 31), Pb 5.1–6.1 μg g^{-1} (mean 2.6), and Zn 48–120 μg g^{-1} (mean 74.7; MDEQ 2006). If the average concentration of copper in tailings is 2860 μg g^{-1}, the discharges released about 74×10^3 kg of copper into Keweenaw Bay. At the current erosion rate (0.069 Tg in year 2008), this corresponds to 198×10^3 kg Cu yr^{-1} loading from just the main pile.

Toxicity of stamp sand environments—In 2003, MDEQ obtained 274 soil samples and 10 groundwater samples from the main ("northern") pile and 24 surface soil samples from redeposited stamp sand piles south of the main pile ("southern site"; MDEQ 2006). At the northern site, the following number of samples exceeded Groundwater Surface Water Interface Criteria (GSWIC) levels. In the 274 soil samples: aluminum 271, chromium 265, cobalt 271, copper 274, manganese 159, nickel 168, silver 216, and zinc 242. In the 10 groundwater samples, the number exceeding the GSWIC risk criteria levels: chromium 5, copper 10, manganese 5, nickel 8, silver 8, and zinc 8. The following 24 surface soil samples exceeded GSWIC levels at the southern site: aluminum 20, chromium 19, cobalt 24, copper 24, manganese 7, nickel 8, silver 9, and zinc 10.

Groundwater seepage through coastal stamp sands is another concern. The reworked beach stamp sands created numerous shallow coastal ponds south of the primary tailings pile (Figs. 2, 8). At Gay, groundwater samples from stamp piles contained Cu concentrations of 670 μg L^{-1}

(Jeong et al. 1999) and 250–22,000 μg L^{-1} (MDEQ 2006). Dissolved Cu concentrations in pond waters ranged between 10 and 2400 μg L^{-1} (Jeong et al. 1999; Lytle 1999). Pond waters were found to be toxic to most aquatic organisms (Kerfoot et al. 1999; Lytle 1999). Native *Daphnia pulex* suspended in Gay stamp sand pools survived only 2–12 d, depending upon local dissolved Cu concentrations. That *Daphnia* would die rapidly is not surprising because toxicity thresholds (LC_{50}) for freshwater organisms usually lie between 25 and 600 μg L^{-1} (ppb) dissolved Cu. Native *D. pulex* were found sensitive to Cu concentrations above 12 μg L^{-1}, i.e., far below existing concentrations in pools (Lytle 1999).

Considerable evidence is also available on copper in sediments contaminated with stamp sands. MDEQ (2006) samples offshore of the Gay stamp sands found copper concentrations in bay sediments varying between 1400 to 4400 μg g^{-1} (mean 3020 μg g^{-1}, $n = 5$). The latter value is very close to pure stamp sands, suggesting little admixture with Tobacco River or Traverse River sediments. Submersed regions immediately around nearshore stamp sand piles on the Keweenaw Peninsula are generally characterized by reduced diversity of benthic macroinvertebrates (Kraft 1979; Kraft and Sypniewski 1981). Freshly worked stamp sand and lake sediments are toxic to *Daphnia* and mayflies (*Hexagenia*) because they release Cu across the pore-water gradient (Malueg et al. 1984). Additional laboratory toxicity experiments with slime-clay–rich lake sediments from the Keweenaw Waterway and Torch Lake showed that solid-phase sediments and aqueous fractions (e.g., interstitial water) associated with the slime-clay sediments were lethal to several taxa of freshwater macroinvertebrates: chironomids (*Chironomus tentans*), oligochaetes (*Lumbriculus variegates*), amphipods (*Hyalella azteca*), and cladocerans (*Ceriodaphnia dubia*). Moreover, the observed toxicity was due to copper, as opposed to other metals (principally zinc and lead) present in the sediments (Schubauer-Berigan et al. 1993; West et al. 1993). However, toxicity to benthic organisms was not predictable based solely on total copper concentrations in the sediments, but appeared related to bio-available copper, the fraction freely dissolved in the sediment interstitial water (Ankley et al. 1993).

Threat to Buffalo Reef and rivers—Buffalo Reef is recognized in the *Atlas of the Spawning and Nursery Areas of the Great Lakes*, Volume 2 (Goodyear et al. 1982). The Great Lakes Indian Fish and Wildlife Commission (GLIFWC) conducted fisheries assessments on the reef between 1986 and 2002, documenting that it is an important spawning reef for whitefish and lake trout (Chiriboga and Mattes 2008). Stamp sand movement is of concern to the Keweenaw Bay tribal council, as tribal members maintain a commercial whitefish and lake trout fishery in Keweenaw Bay. Harvest of these fish is an important cultural and economic activity, as GLIFWC helps tribal members promote and market the health benefits of traditional foods (Mazina'igan 2007). Impairment of reef habitat could lead to a decline in important fish species, infringement upon federally guaranteed treaty reserved rights, and negatively affect the health of the tribal population that consumes these resources. NWRI Shipek grab samples and our Ponar samples in the area immediately north of Buffalo Reef showed the area to have some stamp sands, raising immediate concerns for fish spawning (Biberhofer and Procopec 2008; this investigation). Along the coastline, another concern about shoreline dispersal of stamp sands is interference with migration of fish up streams or rivers for spawning (e.g., rainbow smelt [*Osmerus mordax*], white sucker [*Catostomus commersoni*], rainbow trout "steelhead" [*Oncorhynchus mykiss*]) or impairment of stream or river mouth habitats.

Global concerns about coastal tailings discharges—Between 1850 and 1968, copper ore processing on the Keweenaw Peninsula discharged around 360 Tg of stamp sand tailings along shorelines, connecting waterways, and into interior lakes and rivers (Kerfoot et al. 2009). As mentioned earlier, the Grand Traverse discharges were of such magnitude that they literally changed the shoreline. Ecosystem effects are pervasive, as tailings have now spread along half the above-water beach and $<$ 22-m below-water benthic environments of the bay. Another well-documented Great Lakes case that affected Lake Superior sediments involved discharge of taconite (iron) tailings north of Duluth, Minnesota. Taconite plants mix iron ore with clay, producing a pellet suited for blast furnaces. Most operating mines on the U.S. and Canadian sides are inland, with tailings piles located near open-pit excavations. However, between 1955 and 1980, 500 Mt of taconite tailings were sluiced into Silver Bay, Minnesota. Iron-rich sediments moved into the Duluth Basin, beyond the confines of the 23.3-km^2 permitted dumping site. Small asbestiform particles (cummingtonite) from the discharge subsequently spread along the coast down to the Duluth water intake site and over three western basins of Lake Superior (Duluth, Chefswet, and Thunder Bay Basins). The affected area eventually extended over 100 km from the original discharge site (Cook et al. 1974; IJC 1977; Cook et al. unpubl.). The Clean Water Act of the U.S. and Canada now bans coastal mining discharges. However, lingering effects come from tailings pond failures. At Elliot Lake uranium mining operations, $>$ 30 tailings pond failures were recorded, prompting the International Joint Commission to describe the drainage system as a major source of radium contamination in the Great Lakes (Wynn 2007).

Yet what we discuss here are not historic curiosities confined to the Great Lakes, but rather examples of a substantial problem present around the world. There are numerous cases of past and present mine disposal into freshwater and marine coastal environments (i.e., several examples are listed in Table 5). Coastal disposal sites are widely spread across North America (Canada, U.S.A.), South America (El Salvador, Chile), Northern Europe (Norway, Britain), Mediterranean (Spain, Turkey), Africa, Indonesia, Papua New Guinea, Philippines, and Melanesia (Toga). Despite great expressed concern (Martinez-Frias 1997; Moran et al. 2009), marine coastal deposition continues to be advocated in recent mining methods

Table 5. Mine tailings discharges into coastal environments around the world. Site location, dominant geological mineral property, and publication sources are listed.

Location	Tailings	Years	Dominant metal or mineral	Source
Freda–Redridge, Keweenaw Peninsula, Michigan, U.S.A.	39.2 Tg	1901–1947	Copper	Kerfoot et al. 2009
Gay, Keweenaw Peninsula, Michigan, U.S.A.	22.5 Tg	1901–1932	Copper	Kerfoot et al. 2009
Silver Bay, Minnesota, U.S.A.	500 Tg	1955–1980	Iron	Cook et al. 1974
Rupert Inlet, British Columbia, Canada	353 Tg	1971–1995	Copper	Burd 2002
Britannia Beach, Howe Sound, north of Vancouver, British Columbia, Canada	44 Tg	1904–1974	Copper, zinc	Chretien 1997
Ensenada Chapaco Bay, north-central Chile	2,612,103 kg d^{-1}	1978–1994	Iron tailings (pelletization)	Lancellotti and Stotz 2004
Chanaral Bay, Atacama Region, Chile	150 Tg	1938–1974	Copper, arsenic	Castilla and Nealler 1978; Andrade et al. 2006
Qaumaujuk and Agfardlikavsa Fjords, Greenland	11.8 Tg	1973–1990	Lead, zinc, silver	Asmund et al. 1994
Rize, Black Sea, Turkey	2,880,103 kg d^{-1}	1994–2000	Copper, arsenic, lead	Berkun 2005
Chameis Bay, Namibia, Africa	366 Tg	1970–2006	Diamonds	Smith 2006
Elizabeth Bay, Namibia, Africa	7 Tg	1991–1998	Diamonds	Smith et al. 2002
Calancan Bay, Marinduque Island, Luzon, Philippines	200 Tg	1975–1991	Copper	Marges et al. 2011
Buyat Bay, North Sulawesi, Indonesia	1,841,103 kg d^{-1}	1996–present	Gold	Edinger et al. 2008
Toga, Melanesia, Western Pacific	2.5 Tg yr^{-1}	1990s	Phosphate; Cd, Pb, Cu in tailings	Gnandi et al. 2006

bulletins (Coldwell and Gensler 1993; Ellis and Robertson 1999; Younger 2008).

The incentive for discharging into rivers, embayments, or the ocean goes beyond the old-school engineering ''dilution is the solution.'' Advocacy utilizes the following arguments. On-land tailings disposal generally involves the construction of a dam in stream drainage, or an enclosure on gently sloping terrain, that is used to impound tailings. These containment structures are often the largest surface feature of a mine, flooding hundreds of hectares, and adversely affecting the terrestrial environment. Moreover, tailings impoundments are usually left in place after mining has ceased and require perpetual inspection and maintenance. These impoundments are prone to severe climatic and seismic events, leading to unexpected catastrophic failure and widespread environmental ''catastrophes'' (e.g., ''Aznalcollar Disaster,'' Guadalquivir Estuary, Spain [Grimalt et al. 1999]; ''Marcopper Mining Disaster,'' Calancan Bay, Marinduque Island, Philippines [Marges et al. 2011]). Along the Mediterranean coast, there are $>$ 230 tailings dams in the Spanish province of Almería alone, dating back to Roman times (Martinez-Frias 1997). As an alternative, mining documents suggest that tailings discharged along coastal margins have minimal terrestrial effects and disappear underwater, moving ''out of sight, out of mind.'' Our point is that, unattended, they will move across large regions of bays, greatly expanding environmental effects beyond the area of the original tailings deposition.

Given the global incidence of coastal mine discharges, and concern over how long these effects will play out over extended time periods, one can easily envision how combined LiDAR and MSS or hyperspectral coastal imaging provides valuable information regarding the spread of past mining discharges along shallow stretches of coastal shorelines and ecosystem effects. The ability to discriminate between sediment types has equal value in studies of coastal tailings impoundment failures. However, if the discharges are placed, or move, into waters $>$ 22–35 m, beyond reflectance limits, then alternative tracking methods must be employed. Concerns about stamp sand migration from the Gay pile, aided by preliminary LiDAR and MSS imagery, spurred the United States Army Corps of Engineers Detroit District Office, in February 2011, to approve a US$8–9 million dollar Keweenaw Stamp Sands Ecosystem Restoration Plan for Grand Traverse Bay.

Acknowledgments

The LiDAR project was a collaborative effort between Bruce Sabol and Mark Graves at the Engineer Research and Development Center-Environmental Laboratory (ERDC-EL, Vicksburg, Mississippi), the Joint Airborne LiDAR Bathymetry Technical Center of Expertise (JALBTCX, Kiln, Mississippi), Detroit District Corps of Engineers, faculty and students from Biological Sciences, Chemistry, and Geological Engineering, Mining and Sciences at Michigan Technological University (Michigan Tech, Houghton, Michigan), and research scientists at Michigan Technological Research Center (MTRI; Ann Arbor, Michigan). Primary funding came from the Army Corps of Engineers ERDC-EL laboratory and was provided by the System Wide Water Resources Program (Steve Ashby, program manager) at Vicksburg. Efforts were also aided by a National Science Foundation, Ocean Sciences 97-12872 grant to W.C.K., and a U.S. Environmental Protection Agency Region V Grant to the Baraga Tribal Council passed through to W.C.K. Support for the Compact Hydrographic Airborne Rapid Total Survey (CHARTS) flight and initial data processing was provided by the Corps National Coastal Mapping Program managed by Jennifer Wozencraft at the JALBTCX Center. We also thank Mike Donofrio, Mike Sladewski, Esteban Chiriboga, and especially J. Biberhofer for sharing details of the National

Water Research Institute and Great Lakes Indian Fish and Wildlife Commission sonar mapping and sediment sampling efforts in Grand Traverse Bay. Lucille Zelazny aided preparation of figures, and Jamey Anderson sieved stamp sand samples.

References

Ackermann, F. 1999. Airborne laser scanning—present status and future expectations. J. Photogram. Remote Sens. **54:** 64–67, doi:10.1016/S0924-2716(99)00009-X

Andrade, S., J. Moffett, and J. A. Correa. 2006. Distribution of dissolved species and suspended particulate copper in an intertidal ecosystem affected by copper mine tailings in Northern Chile. Mar. Chem. **101:** 203–212, doi:10.1016/j.marchem.2006.03.002

Ankley, G. T., V. R. Mattson, E. N. Leonard, C. W. West, and J. L. Bennett. 1993. Predicting the acute toxicity of copper in freshwater sediments: Evaluation of the role of acid volatile sulfide. Environ. Toxicol. Chem. **11:** 315–320, doi:10.1002/etc.5620120214

Asmund, G., P. G. Broman, and G. Lindgren. 1994. Managing the environment at the Black Angel Mine, Greenland. Int. J. Surf. Min., Reclam. Environ. **8:** 37–40, doi:10.1080/09208119408964755

Benedict, C. H. 1952. Red metal: The Calumet and Hecla story. Univ. of Michigan Press.

———. 1955. Lake Superior milling practice. Michigan College of Mining and Technology.

Berkun, M. 2005. Submarine tailings placement by a copper mine in the deep anoxic zone of the Black Sea. Water Res. **39:** 5005–5016, doi:10.1016/j.watres.2005.10.005

Biberhofer, J., and C. M. Prokopec. 2008. Delineation and characterization of aquatic substrate features on or adjacent to Buffalo Reef, Keweenaw Bay, Lake Superior. Technical Note AERMB-TN06. Environment Canada National Water Resource Institute.

Bowen, Z. H., and R. G. Waltermire. 2002. Evaluation of light distancing and ranging (LiDAR) for measuring river corridor topography. J. Am. Water Resour. Assoc. **38:** 33–41, doi:10.1111/j.1752-1688.2002.tb01532.x

Brock, J., C. Wright, A. Sallenger, W. Krabill, and R. Swift. 2002. Basis and methods of NASA Airborne Topographic Mapper lidar surveys for coastal studies. J. Coast. Res. **18:** 1–13.

Brock, J. C., C. W. Wright, T. D. Clayton, and A. Nayegandhi. 2004. LIDAR optical rugosity of coral reefs in Biscayne National Park, Florida. Coral Reefs **23:** 48–59, doi:10.1007/s00338-003-0365-7

Budd, J., W. C. Kerfoot, D. Pilant, and L. M. Jipping. 1999. The Keweenaw Current and ice rafting: Use of satellite imagery to investigate copper-rich particle dispersal. J. Great Lakes Res. **25:** 642–662, doi:10.1016/S0380-1330(99)70768-9

Burd, B. J. 2002. Evaluation of mine tailings effects on a benthic marine infaunal community over 29 years. Mar. Environ. Res. **53:** 481–519, doi:10.1016/S0141-1136(02)00092-2

Butler, B. S., and W. S. Burbank. 1929. The copper deposits of Michigan. Professional Paper 144. United States Geological Survey.

Castilla, J. C., and E. Nealler. 1978. Marine environmental impact due to mining activities of El Salvador copper mine, Chile. Mar. Pollut. Bull. **9:** 67–70, doi:10.1016/0025-326X(78)90451-4

Chen, C., J. Zhu, E. Ralph, S. A. Green, J. Wells Budd, and F. Y. Zhang. 2001. Prognostic modeling studies of the Keweenaw Current in Lake Superior. Part I: Formation and evolution. J. Phys. Oceanogr. **31:** 379–395, doi:10.1175/1520-0485(2001)031<0379:PMSOTK>2.0.CO;2

Chiriboga, E. D., and W. P. Mattes. 2008. Buffalo Reef and substrate mapping project. Administrative Report 08-04. Great Lakes Indian Fish and Wildlife Indian Commission.

Coldwell, J. R., and E. C. Gensler. 1993. Potential for submarine tailings disposal to affect the availability of minerals from United States coastal areas. OFR 101-93. U.S. Bureau of Mines.

Cook, P. M., G. E. Glass, and J. H. Tucker. 1974. Asbestiform amphibole minerals: Detection and measurement of high concentrations in municipal water supplies. Science **185:** 853–855, doi:10.1126/science.185.4154.853

Chretien, A. R. 1997. Geochemical behaviour, fate and impact of Cu, Cd, and Zn from mine effluent discharging in Howe Sound. Ph.D. thesis. Univ. of British Columbia.

Crow, P., S. Benham, B. J. Devereux, and G. S. Amable. 2007. Woodland vegetation and its implications for archaeological survey using LiDAR. Forestry **80:** 241–252, doi:10.1093/forestry/cpm018

Edinger, E. N., K. Azmy, W. Diegor, and P. R. Siregar. 2008. Heavy metal contamination from gold mining recorded in *Porites lobata* skeletons, Buyat-Ratototok district, North Sulawesi, Indonesia. Mar. Pollut. Bull. **56:** 1553–1569, doi:10.1016/j.marpolbul.2008.05.028

Ellis, D. V., and J. D. Robertson. 1999. Underwater placement of mine tailings: Case examples and principles, p. 123–141. *In* J. M. Azcue [ed.], Environmental impacts of mining activities. Springer. p. 123–141.

Gewurtz, S. B., L. Shen, P. A. Helm, J. Waltho, E. J. Reiner, S. Painter, I. D. Brindle, and C. H. Marvin. 2008. Spatial distributions of legacy contaminants in sediments of lakes Huron and Superior. J. Great Lakes Res. **34:** 153–168, doi:10.3394/0380-1330(2008)34[153:SDOLCI]2.0.CO;2

Gnandi, K., G. Tchangbedji, K. Killi, G. Baba, and K. Abbe. 2006. The impact of phosphate mine tailings on the bioaccumulation of heavy metals in marine fish and crustaceans from the coastal zone of Togo. Mine Water Environ. **25:** 56–62, doi:10.1007/s10230-006-0108-4

Goodyear, C. S., T. A. Edsall, D. M. Ormsby Dempsey, G. D. Moss, and P. E. Polanski. 1982. Atlas of the spawning and nursery areas of Great Lakes fishes. U.S. FWS/OBS-82/52. U.S. Fish and Wildlife Service.

Grimalt, J. O., M. Ferrer, and E. Macpherson. 1999. The mine tailing accident in Aznalcollar. Sci. Total Environ. **242:** 3–11.

Guenther, G. C. 2007. Airborne lidar bathymetry, p. 253–320. *In* D. F. Maune [ed.], Digital elevation model technologies and applications: The DEM users manual, 2nd ed. American Society for Photogrammetry and Remote Sensing. p. 253–320.

Hedley, J. D., A. R. Harborne, and P. J. Mumby. 2005. Simple and robust removal of sun glint for mapping shallow-water benthos. Int. J. Remote Sens. **26:** 2107–2112, doi:10.1080/01431160500034086

International Joint Commission, 1977. Great Lakes Water Quality, 1977 Annual Report. Great Lakes Water quality Board. Windsor, Ontario.

Jensen, J. R. 2004. Introductory digital image processing: A remote sensing perspective, 3rd ed. Prentice Hall PTR.

Jeong, J., and D. McDowell. 2003. Characterization and transport of contaminated sediments in the southern central Lake Superior. J. Miner. Mater. Charact. Eng. **2:** 111–135.

———, N. R. Urban, and S. Green. 1999. Release of copper from mine tailings on the Keweenaw Peninsula. J. Great Lakes Res. **25:** 721–734, doi:10.1016/S0380-1330(99)70772-0

Johnston, J. W., T. A. Thompson, and S. J. Baedke. 2000. Preliminary report of Late Holocene lake-level variation in southern Lake Superior: Part 1. Indiana Geological Survey, Open File Study 99-18. Indiana Univ.

Kerfoot, W. C., S. Harting, R. Rossmann, and J. A. Robbins. 1999. Anthropogenic copper inventories and mercury profiles from Lake Superior: Evidence for mining impacts. J. Great Lakes Res. **25:** 663–682, doi:10.1016/S0380-1330(99)70769-0

———, S. L. Harting, J. Jeong, J. A. Robbins, and R. Rossmann. 2004. Local, regional and global implications of elemental mercury in metal (copper, silver, gold, and zinc) ores: Insights from Lake Superior sediments. J. Great Lakes Res. **52:** 162–184, doi:10.1016/S0380-1330(04)70384-6

———, ———, R. Rossmann, and J. A. Robbins. 2002. Elemental mercury in copper, silver and gold ores: An unexpected contribution to Lake Superior sediments with global implications. Geochem. Explor. Environ. Anal. **2:** 185–202, doi:10.1144/1467-787302-022

———, J. Jeong, and J. A. Robbins. 2009. Lake Superior mining and the proposed Mercury Zero-discharge Region, p. 153–216. *In* M. Munawar [ed.], State of Lake Superior. Ecovision World Monograph Series. p. 153–216.

———, G. Lauster, and J. A. Robbins. 1994. Paleolimnological study of copper mining around Lake Superior: Artificial varves from Portage Lake provide a high resolution record. Limnol. Oceanogr. **39:** 649–669, doi:10.4319/lo.1994.39.3.0647

———, and J. A. Robbins. 1999. Nearshore regions of Lake Superior: Multi-element signatures of mining discharges and a test of Pb-210 deposition under conditions of variable sediment mass flux. J. Great Lakes Res. **25:** 697–720, doi:10.1016/S0380-1330(99)70771-9

Kolak, J. J., D. T. Long, W. C. Kerfoot, T. M. Beals, and S. J. Eisenreich. 1999. Nearshore versus offshore copper loading in Lake Superior sediments: Implications for transport and cycling. J. Great Lakes Res. **25:** 611–624, doi:10.1016/S0380-1330(99)70766-5

Kraft, K. J. 1979. *Pontoporeia* distribution along the Keweenaw shore of Lake Superior affected by copper tailings. J. Great Lakes Res. **7:** 258–263, doi:10.1016/S0380-1330(81)72053-7

———, and R. H. Sypniewski. 1981. Effect of sediment copper on the distribution of benthic macroinvertebrates in the Keweenaw Waterway. J. Great Lakes Res. **7:** 258–263, doi:10.1016/S0380-1330(81)72053-7

Lam, D. C. 1978. Simulation of water circulation and chloride transports in Lake Superior for summer 1973. J. Great Lakes Res. **4:** 343–349, doi:10.1016/S0380-1330(78)72203-3

Lancellotti, D. A., and W. B. Stotz. 2004. Effects of shoreline discharge of iron mine tailings on a marine soft-bottom community in northern Chile. Mar. Pollut. Bull. **48:** 303–312, doi:10.1016/j.marpolbul.2003.08.005

Lefsky, M. A., D. Harding, W. B. Cohen, G. Parker, and H. H. Shugart. 1999. Surface lidar remote sensing of basal area and biomass in deciduous forests of eastern Maryland, USA. Remote Sens. Environ. **67:** 83–98.

Lytle, R. D. 1999. In situ copper toxicity tests: Applying likelihood ratio tests to *Daphnia pulex* incubations in Keweenaw Peninsula waters. J. Great Lakes Res. **25:** 744–759, doi:10.1016/S0380-1330(99)70774-4

Lyzenga, D. R. 1981. Remote sensing of bottom reflectance and water attenuation parameters in shallow water using aircraft and Landsat data. Int. J. Remote Sens. **2:** 71–82, doi:10.1080/01431168108948342

Macdonald, R. W., B. Morton, and S. C. Johannessen. 2003. A review of marine environmental contaminant issues in the North Pacific: The dangers and how to identify them. Environ. Rev. **11:** 103–139, doi:10.1139/a03-017

Malueg, K. W., G. S. Schuytema, D. F. Krawczyk, and J. H. Gakstatter. 1984. Laboratory sediment toxicity tests, sediment chemistry and distribution of benthic macroinvertebrates in sediments from the Keweenaw Waterway, Michigan. Environ. Toxicol. Chem. **3:** 233–242, doi:10.1002/etc.5620030206

Marges, M., G. S. Su, and E. Ragragio. 2011. Assessing heavy metals in the waters and soils of Calancan Bay, Marinduque Island, Philippines. J. Appl. Sci. Environ. Sanit. **6:** 45–49.

Martinez-Frias, J. 1997. Mine waste pollutes Mediterranean. Nature **388:** 120, doi:10.1038/40506

Mazina'igan. 2007. A chronicle of the Lake Superior Ojibwe, 2007 summer edition. Great Lakes Fish and Wildlife Commission.

MDEQ. 2006. Toxicological evaluation for the Gay, Michigan stamp sand. W.O. No. 20083.032.00. Weston Solutions.

Monette, C. J. 1992. Upper peninsula's wolverine. Welden H. Curtin, Lake Linden, Michigan.

Moran, R., A. Reichelt-Brushett, and R. Young. 2009. Out of sight, out of mine: Ocean dumping of mine wastes; the world's oceans, already imperiled, face a new threat. WorldWatch **22**, (2), 30–34.

Murdoch, W. A. 1943. Boom copper: The story of the first United States mining boom. Macmillan.

Nayegandhi, A., J. C. Brock, and C. W. Wright. 2005. Classifying vegetation using NASA's Experimental Advanced Airborne Research Lidar (EAARL) at Assateague Island National Seashore [CD-ROM]. *In* American Society of Photometry and Remote Sensing Annual Conference Proceedings. American Society of Photometry and Remote Sensing.

Rasmussen, T., R. Fraser, D. S. Lemberg, and R. Regis. 2002. Mapping stamp sand dynamics: Gay, Michigan. J. Great Lakes Res. **28:** 276–284, doi:10.1016/S0380-1330(02)70583-2

Sabol, B., E. Lord, K. Reine, and D. Shafer. 2008. Comparison of acoustic and aerial photographic methods for quantifying the distribution of submersed aquatic vegetation in Sagamore Creek, NH. DOER-E23. U.S. Army Engineer Research and Development Center.

Schubauer-Berigan, M. K., J. R. Dierkes, P. D. Monson, and G. T. Ankley. 1993. pH-dependent toxicity of Cd, Cu, Ni, Pb, and Zn to *Ceriodaphnia dubia*, *Pimephales promelas*, *Hyalella azteca* and *Lumbriculus variegates*. Environ. Toxic. Chem. **12:** 1261–1266.

Smith, G., G. Mocke, R. van Ballegooyen, and C. Soltau. 2002. Consequences of sediment discharge from dune mining at Elizabeth Bay, Namibia. J. Coast. Res. **18:** 776–791.

Smith, G. G. 2006. Assessment of the cumulative effects of sediment discharges from on-shore and near-shore diamond mining activities on the BCLME. CSIR, Natural Resources and the Environment.

Urban, N. R., X. Lu, Y. Chai, and D. S. Apul. 2004. Sediment trap studies in Lake Superior: Insights into resuspension, cross-margin transport, and carbon cycling. J. Great Lakes Res. **30:** 147–161, doi:10.1016/S0380-1330(04)70383-4

West, C. W., V. R. Mattson, E. N. Leonard, G. L. Phipps, and G. T. Ankley. 1993. Comparison of the relative sensitivity of three benthic invertebrates to copper contaminated sediments from the Keweenaw Waterway. Hydrobiologia **262:** 57–68, doi:10.1007/BF00010989

Weston. 2007. Migrating Stamp Sand Mitigation Plan technical evaluation. Prepared for MDEQ, Remediation and Redevelopment Division, Calumet Field Office. Weston Solutions of Michigan.

Wynn, G. 2007. Canada and arctic North America: An environmental history. ABC-CILO.

YOUNGER, P. L. 2008. Towards regulatory criteria for discharging iron-rich mine water into the sea. Mine Water Environ. **27:** 56–61, doi:10.1007/s10230-007-0027-z

ZHU, J., C. CHEN, E. RALPH, S. A. GREEN, J. W. BUDD, AND F. Y. ZHANG. 2001. Prognostic modeling studies of the Keweenaw Current in Lake Superior. Part II: Simulation. J. Phys. Oceanogr. **31:** 396–410, doi:10.1175/1520-0485(2001)031<0396:PMSOTK>2.0.CO;2

Associate editor: Dariusz Stramski

Received: 28 April 2011
Accepted: 28 November 2011
Amended: 02 February 2012